Supporting Information

Photo-activation of MDM2-inhibitors: Controlling Protein-Protein Interaction with Light.

Mickel J. Hansen[1,ϕ], Femke M. Feringa[2, ϕ], Piermichele Kobauri[1], Wiktor Szymanski[1,3], René H. Medema[2] and Ben L. Feringa[1*]*

[1]Centre for Systems Chemistry, Stratingh Institute for Chemistry, University of Groningen, Nijenborgh 4, 9747 AG, Groningen, The Netherlands.

[2]Oncode Institute, Netherlands Cancer Institute, Division of Cell Biology, Amsterdam 1066 CX, The Netherlands.

[3]Department of Radiology, University Medical Center Groningen, University of Groningen, Hanzeplein 1, 9713GZGroningen, The Netherlands

[ϕ]These authors contributed equally.

Materials and Methods

General. All chemicals for synthesis were obtained from commercial sources and used as received unless stated otherwise.

Thin Layer Chromatography (TLC) was performed using commercial Kieselgel 60, F254 silica gel plates with fluorescence-indicator UV_{254} (*Merck*, TLC silica gel *60 F_{254}*). For detection of components, UV light at λ = 254 nm or λ = 365 nm was used. Alternatively, oxidative staining using aqueous basic potassium permanganate solution ($KMnO_4$) or aqueous acidic cerium phosphomolybdic acid solution (Seebach's stain) was used. Flash chromatography was performed on silica gel (Silicycle Siliaflash P60, 40-63 mm, 230-400 mesh). Drying of solutions was performed with $MgSO_4$ and volatiles were removed with a rotary evaporator. Nuclear Magnetic Resonance spectra were measured with an Agilent Technologies 400-MR (400/54 Premium Shielded) spectrometer (400 MHz). All spectra were measured at room temperature (22–24 °C). Chemical shifts for ^{1}H- and ^{13}C-NMR measurements were determined relative to the residual solvent peaks in ppm (δ_H 7.26 for $CHCl_3$, 2.50 for DMSO and 2.05 ppm for Acetone, δ_C 77.16 for $CHCl_3$ and 39.52 for DMSO). The following abbreviations are used to indicate signal multiplicity: s, singlet; d, doublet; t, triplet; q, quartet; m, multiplet; brs, broad signal. All ^{13}C-NMR spectra are ^{1}H-broadband decoupled. High-resolution mass spectrometric measurements were performed on a Thermo scientific LTQ Orbitrap XL with ESI ionization. For spectroscopic measurements, solutions in Uvasol® grade solvents were measured in a 10 mm quartz cuvette. UV-Vis absorption spectra were recorded on an Agilent 8453 UV-Visible absorption Spectrophotometer.

Chemical actinometry and quantum yield determination

An aqueous 0.05 m H_2SO_4 solution containing 12 mM $K_3[Fe(C_2O_4)_3]$ (3 mL, 1 cm quartz cuvette) was irradiated at 20 °C for a given period of time in the dark with the 400 nm light. A volume of 10 μL was taken and diluted to 2.0 mL with an aqueous 0.5 m H_2SO_4 solution containing phenanthroline (1 g/L) and NaOAc (122.5 g/L). The absorption at λ= 517 nm was measured and compared to an identically prepared non-irradiated sample. The concentration of $[Fe(phenanthroline)_3]^{2+}$ complex was calculated using its molar absorptivity ($\mathcal{E}$ = 20489 m^{-1} cm^{-1}).[1] This concentration corresponded to the concentration of Fe^{2+} ions that had formed upon irradiation divided by 200. The Fe^{2+} ion concentration was plotted versus time and the following slope, obtained by linear fitting to the equation y = ax +b using Origin software, equals the rate of formation for the given wavelength at standardized conditions. This rate can be converted in light doses by taking into account the quantum yield and area of irradiation which is 3 cm^2 for the 400 nm irradiation. Subsequently, the energy per moles of photons at a given wavelength ($E_{mole\ of\ photons} = N_A \times h \times \nu = N_A \times h \times c / \lambda$) is taken to convert this into J s^{-1} cm^{-2}.

A solution of compound **8** was irradiated with the 400 nm Sahlmann LED under identical standardized conditions as with the actinometry at concentrations high enough to absorb all incident light (absorbance at 400 nm ≥ 2). The absorbance increase at λ = 420 nm was monitored over time by UV-vis spectroscopy. The molar absorptivities at = 400 nm [For compound **8**, $\mathcal{E}_8$ = 20489 m^{-1} cm^{-1}; for compound **6**, $\mathcal{E}_6$ = 11577 m^{-1} cm^{-1}] were used to calculate the concentration decrease of compound **8** according to $\Delta c = \Delta abs/(\mathcal{E}_8 + \mathcal{E}_6)$. The initial concentration increase was plotted versus time and the slope, the rate of photocleavage of compound **8** over time, including standard error, was obtained by linear fitting to the equation y = ax +b using Origin software. The photochemical quantum yield for **8** (ϕ_8) was calculated by comparison of the rate of photocleavage with the rate of Fe^{2+} ion formation at identical conditions upon 400 nm irradiation from potassium ferrioxalate using the known quantum yield for the ferrioxalate at the given wavelength (ϕ= 1.14).[2]

Cell culture

hTert-immortalized retinal pigment epithelium (RPE-1) cells (ATCC) and hTert-immortalized BJ cells were maintained in Dulbecco's Modified Eagle Medium/Nutrient Mixture F-12 (DMEM/F12, Gibco) supplemented with ultraglutamine, penicillin/streptomycin and 10% fetal calf serum. RPE-1 cells with a fluorescently tagged version of p53 (p53-venus) were a kind gift from the *Lahav* lab.[3] RKO coloncarcinoma cells were maintained in Dulbecco's Modified Eagle Medium (DMEM, Gibco) supplemented with ultraglutamine, penicillin/streptomycin and 10% fetal calf serum. U2OS cells were maintained in Dulbecco's Modified Eagle Medium (DMEM, Gibco) supplemented with ultraglutamine, penicillin/streptomycin and 6% fetal calf serum.

Immunofluorescent staining and live cell imaging

RPE-1 cells were plated on coverslips at equal density and treated with indicated drugs before -/+ irradiation (400 nm for 5 min). For immune fluorescent staining, cells were fixed 4 h after irradiation by wash out of the medium, single wash in phosphate-buffered saline (1x PBS) and incubation in 3.7% formaldehyde for 5 min. Next, fixed cells were permeabilized with 0,2% TritonX in 1x PBS for 5 min before blocking in 3% fetal bovine serum (BSA) in 1× PBS supplemented with 0,1% Tween (PBST) for 1 h (all at room temperature (RT)). Cells were incubated overnight at 4 °C with primary antibody in PBST with 3% BSA, washed three times with PBST, and incubated with secondary antibody and DAPI in PBST with 3% BSA for 2h at RT. After a final three time wash with PBST coverslips were mounted on microscopic analysis slides using ProLong Gold antifade reagent (Thermo Fisher). The following antibodies were used: anti-p53 (sc-126, Santa Cruz, 1/1000), phalloidin (A12380, Molecular Probes, 1/1000) and goat anti-mouse/Alexa 488 (A11029, Molecular Probes, 1/1000).
For live cell imaging cells were grown in picovitro microwells covered by a silicon membrane[4] in Leibovitz's L-15 (Gibco) CO_2-independent medium supplemented with ultraglutamine, penicillin/streptomycin and 10% fetal calf serum. Images for both fixed slides and live cell imaging were obtained using a Delta Vision Elite (applied precision) equipped with a 60X 1.6 NA or 10X 0.75 NA lens (Olympus) and cooled CoolSnap CCD camera. Directed laser irradiation was performed using a brief (0.1 s) pulse of a 405nm laser on the Delta Vision Elite microscope equipped with a X4 laser module (Applied Precision). Image analysis was done using ImageJ software. Automated single cell analysis from live cell imaging was done as described before.[5]

Western Blot

RPE-1 cells were plated at equal density in 6-well plates followed by indicated treatments -/+ irradiation (400 nm for 5 min) 24h later. Cells were fixed and collected 4h after treatment by wash out of the medium, single wash in 1x PBS followed by addition of laemmli buffer (4% SDS, 20% glycerol and 0.125 M Tris HCl). Equal amounts of proteins were separated by SDS-PAGE electrophoresis followed by semi-dry transfer to a nitrocellulose membrane. Membranes were blocked in 5% milk in PBST for 1h at RT before overnight incubation with primary

antibody in PBST with 3% BSA at 4 °C. Membranes were washed 3 times with PBST followed by incubation with secondary antibody in PBST with 5% milk for 2h at RT. Antibody staining was visualized using ECL (GE Healthcare). The following primary antibodies were used: anti-p53 (sc-126, Santa Cruz, 1/1000), anti-Cdk4 (C-22) (sc-260, Santa Cruz, 1/1000). Peroxidase-conjugated- goat anti-mouse (P0447 DAKO, 1/1000) and goat anti-rabbit (P448 DAKO, 1/1000) were used as secondary antibodies.

Colonogenic outgrowth

Cells were plated at equal amounts (1000 cells per well) in a 24-wells plate followed by indicated treatments -/+ irradiation (400 nm for 5 min) 24h later. Cells were cultured under normal cell culture conditions for 6 days to allow colony outgrowth. Plates were fixed using 99.8% ice-cold methanol (Honeywell) for 10 min at RT. After a 1 time wash in H_2O, cells were incubated in 0,2% crystal violet (Sigma) in H_2O for at least 3h at RT to stain cellular outgrowth.

Molecular docking

All calculations were performed on a HP EliteDesk, having an Intel Core i7-6700 processor with four cores, AMD Radeon R9 350 graphic card, using the modelling software Maestro, version 11.3. All the images were obtained with Pymol 2.0.5.

Since no crystal structure of MDM2 complexed with idasanutlin is available, the binding mode of a highly similar pyrrolidine inhibitor (PDB: 4JRG)[6] was used as a reference.

The protein was prepared through the Protein Preparation Wizard in Maestro: this tool interactively allows the assignment of bond orders, hydrogen addition, hydrogen bond definition and optimization, water removal and restrained minimization with OPLS3 force field. All water molecules were removed except for three and two molecules in chain A and B, respectively, that were judged important for the binding mode prediction because of hydrogen bonds with the pyrrolidine head. The grid was created through the Receptor Grid Generation, picking the ligand to define the centroid of the receptor box.

MacroModel was used to minimize the ligands (force field: OPLS3, solvent: water, method: TNCG with 2500 maximum iterations), and to create conformers (same settings as above, conformational search method: Mixed torsional/Low-mode sampling). These conformers were docked with Glide XP, flexible, writing out at most 5 poses per ligand and performing post-docking minimization. Glide gscore was used as the scoring function.

Redocking of the co-crystallized ligand was carried out on chains A and B, both with and without the above-mentioned water molecules. The best result (RMSD=1.284) was achieved with chain A including the bridging water molecules (Figure S1), therefore this was the structure of choice for the further optimization. As with other nutlin analogues, the 4-chloro-phenyl ring fits to the Trp23 and Leu26 pockets, while the neopentyl group occupies the Phe19 pocket near Met62. A hydrogen bond is formed between the amide and His92, and three water molecules mediate the interaction between the pyrrolidine ring and Gln55 and Tyr51.

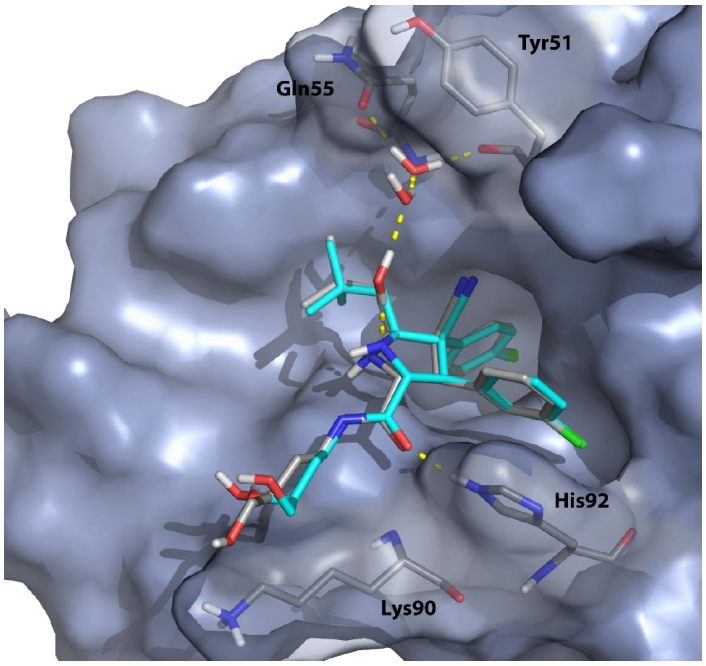

Figure S1: Redocking (grey) of co-crystallized ligand from PDB 4JRG (cyan). Hydrogen bonds are depicted as yellow dashed lines.

Docking of idasanutlin resulted in poses that were very similar to the co-crystallized ligand (Figure S2) and suggested a solvent-exposed salt bridge between the carboxylate group and Lys90 (3.9 Å), which was consistent across all the predicted binding modes. The PPG-idasanutlin docking poses showcased the great flexibility of the photoprotecting group part of the chain (Figure S3), which gave only non-specific interactions with the outer surface of MDM2, including a sub-optimal (not linear and highly solvent-exposed) hydrogen bond between Lys90 and the lactone of the coumarin PPG. Protection of *m*-methoxybenzoic acid blocks the salt bridge formation and causes the miscellaneous positioning of coumarin (Figure S4).

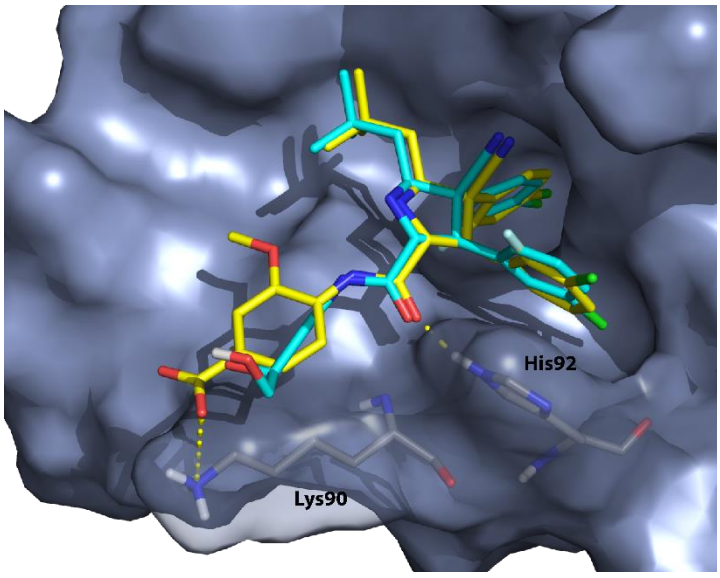

Figure S2: Docking of idasanutlin (yellow) compared to the co-crystallized ligand from PDB 4JRG (cyan). Hydrogen bond and salt bridge are depicted as yellow dashed lines.

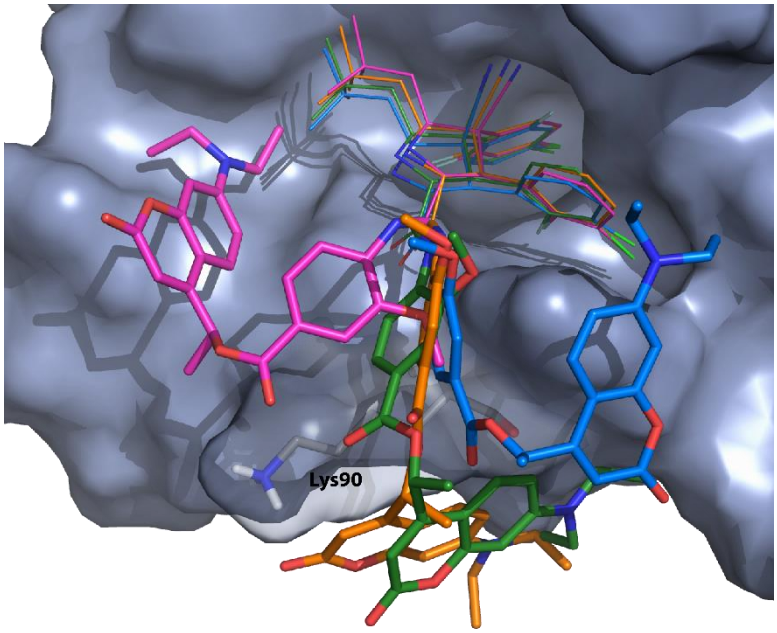

Figure S3: Relevant docking poses of PPG-idasanutlin. The cores are represented as lines until the amide bond, while the remaining parts are showed as sticks.

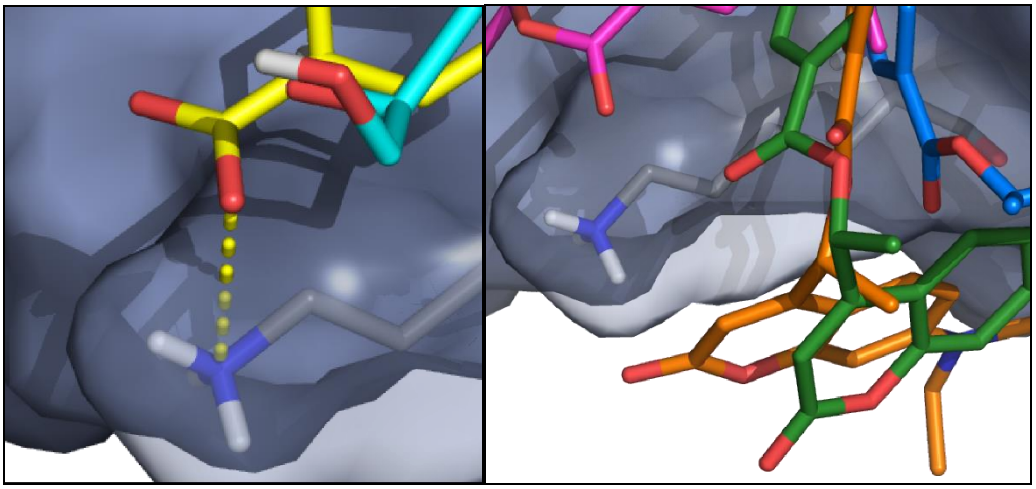

Figure S4: Comparison of the area surrounding Lys90 after docking of idasanutlin (left) and PPG-idasanutlin (right).

Synthesis

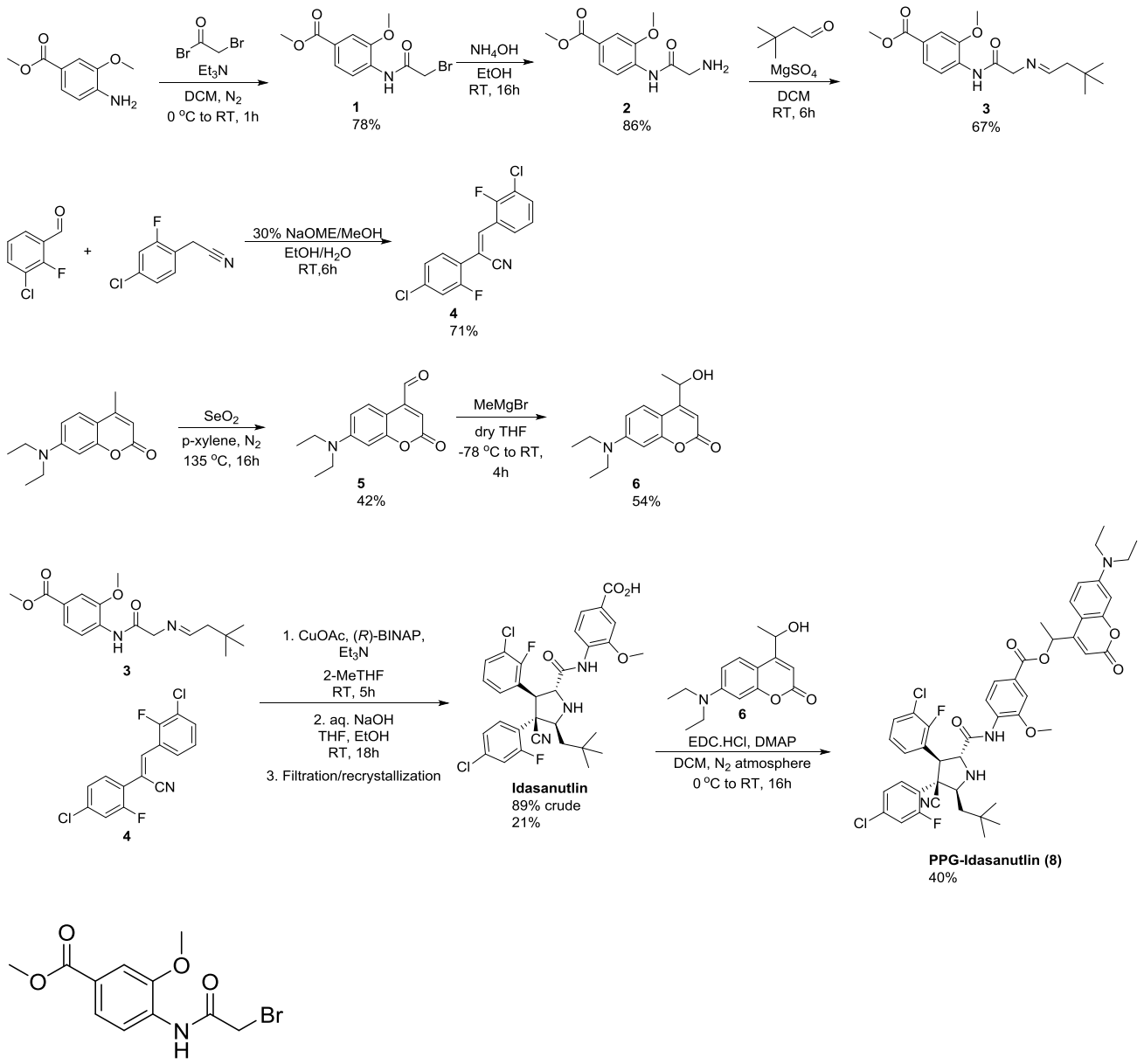

methyl 4-(2-bromoacetamido)-3-methoxybenzoate (**1**)

To a solution of methyl 4-amino-3-methoxybenzoate (500 mg, 2.76 mmol) in DCM (18 mL) at 0 °C was added Et_3N (768 µL, 5.52 mmol) under N_2 atmosphere. Subsequently, 2-bromoacetyl-bromide (610 mg, 263 µL, 3.03 mmol) was slowly added and the reaction mixture was stirred for 45 min at 0 °C. Subsequently, 1M aq. HCl (10 mL) was added and the solution was extracted with DCM (2 x 20 mL). The organic layers were washed with sat. aq. $NaHCO_3$ (20 mL) and brine (20 mL) and dried ($MgSO_4$). Evaporation of the volatiles *in vacuo* and recrystallization from EtOH and MeCN yielded the pure product (654 mg, 78%).

^{1}H NMR (400 MHz, $CDCl_3$): δ 8.95 (s, 1H), 8.41 (d, *J* = 8.5 Hz, 1H), 7.70 (dd, *J* = 8.5, 1.8 Hz, 1H), 7.57 (d, *J* = 1.8 Hz, 1H), 4.04 (s, 2H), 3.98 (s, 3H), 3.91 (s, 3H).

^{13}C NMR (100 MHz, $CDCl_3$): δ 166.6, 163.5, 147.7, 131.0, 125.9, 123.2, 118.4, 110.8, 56.1, 52.1, 29.5.

^{1}H-NMR:

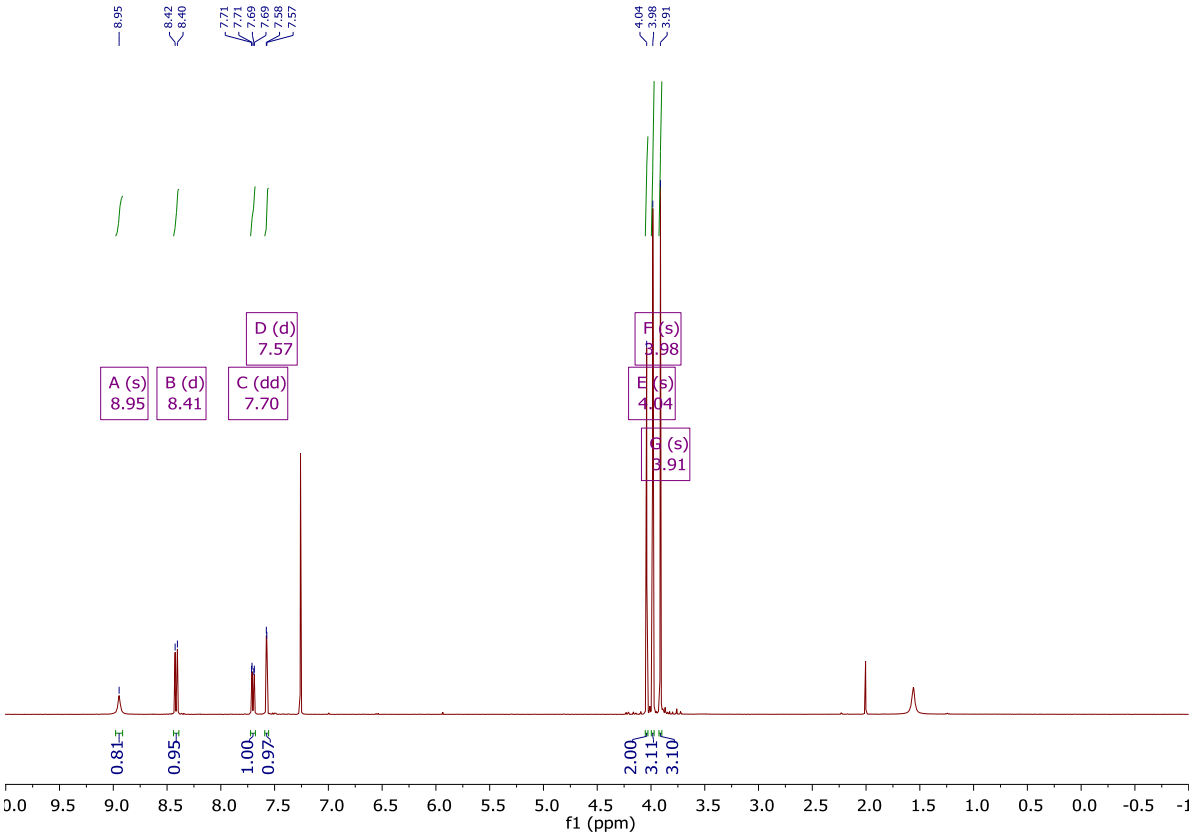

^{13}C-NMR:

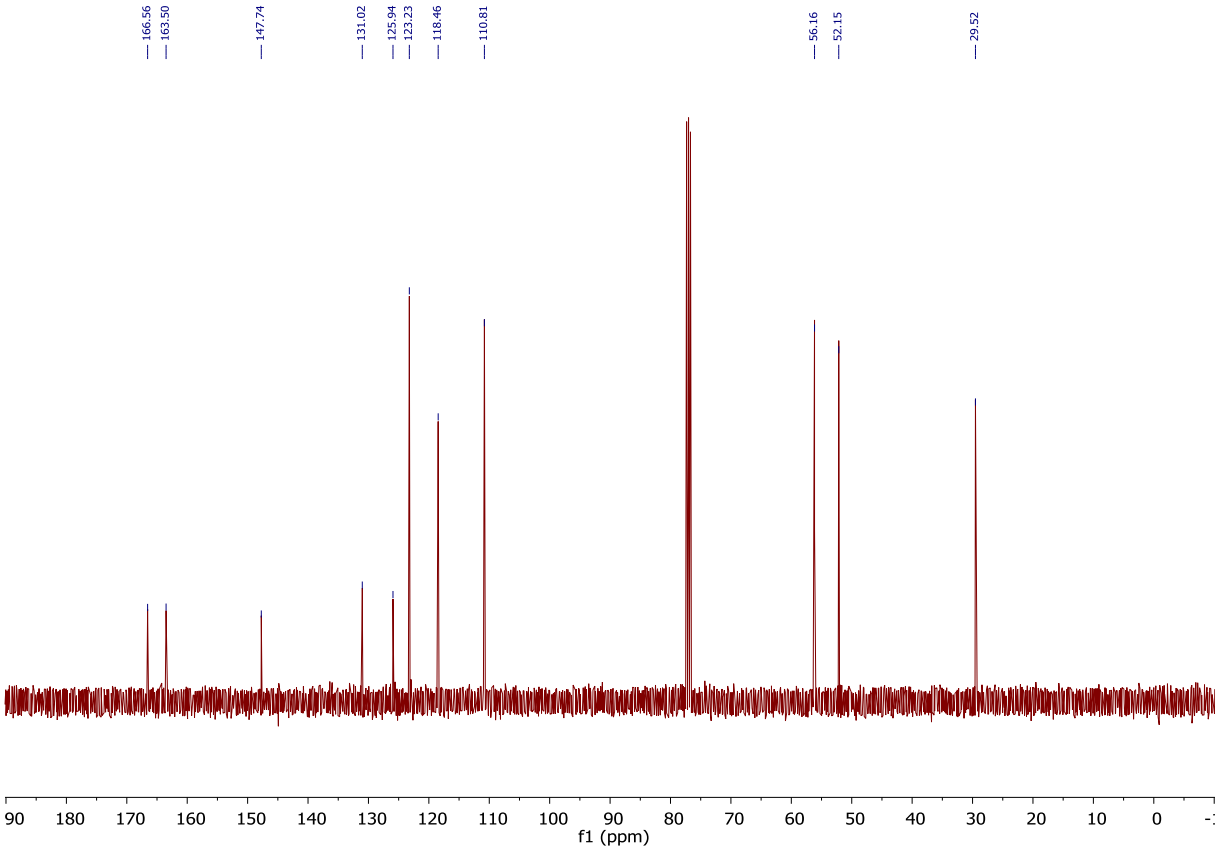

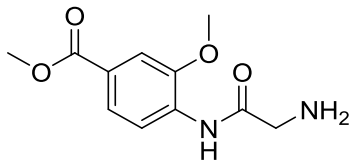

methyl 4-(2-aminoacetamido)-3-methoxybenzoate (**2**)

To an aqueous solution of NH_3 (20 mL) was slowly (dropwise) added **1** (1.40 g, 4.63 mmol) in EtOH (45 mL) in 30 min. Subsequently, the reaction was stirred for 5h at RT and extracted with DCM (3 x 50 mL). The organic layers were washed with brine (3 x 50 mL) and dried ($MgSO_4$). Evaporation of the volatiles *in vacuo* yielded the pure product (945 mg, 86%).

^{1}H NMR (400 MHz, $CDCl_3$): δ 10.00 (s, 1H), 8.52 (d, *J* = 8.5 Hz, 1H), 7.69 (dd, *J* = 8.4, 1.8 Hz, 1H), 7.56 (d, *J* = 1.8 Hz, 1H), 3.96 (s, 3H), 3.90 (s, 3H), 3.52 (s, 2H). Data in accordance with literature.[7]

^{13}C NMR (100 MHz, $CDCl_3$): δ 171.2, 166.7, 147.7, 131.6, 124.9, 123.3, 118.3, 110.7, 55.9, 52.0, 45.6.

^{1}H-NMR:

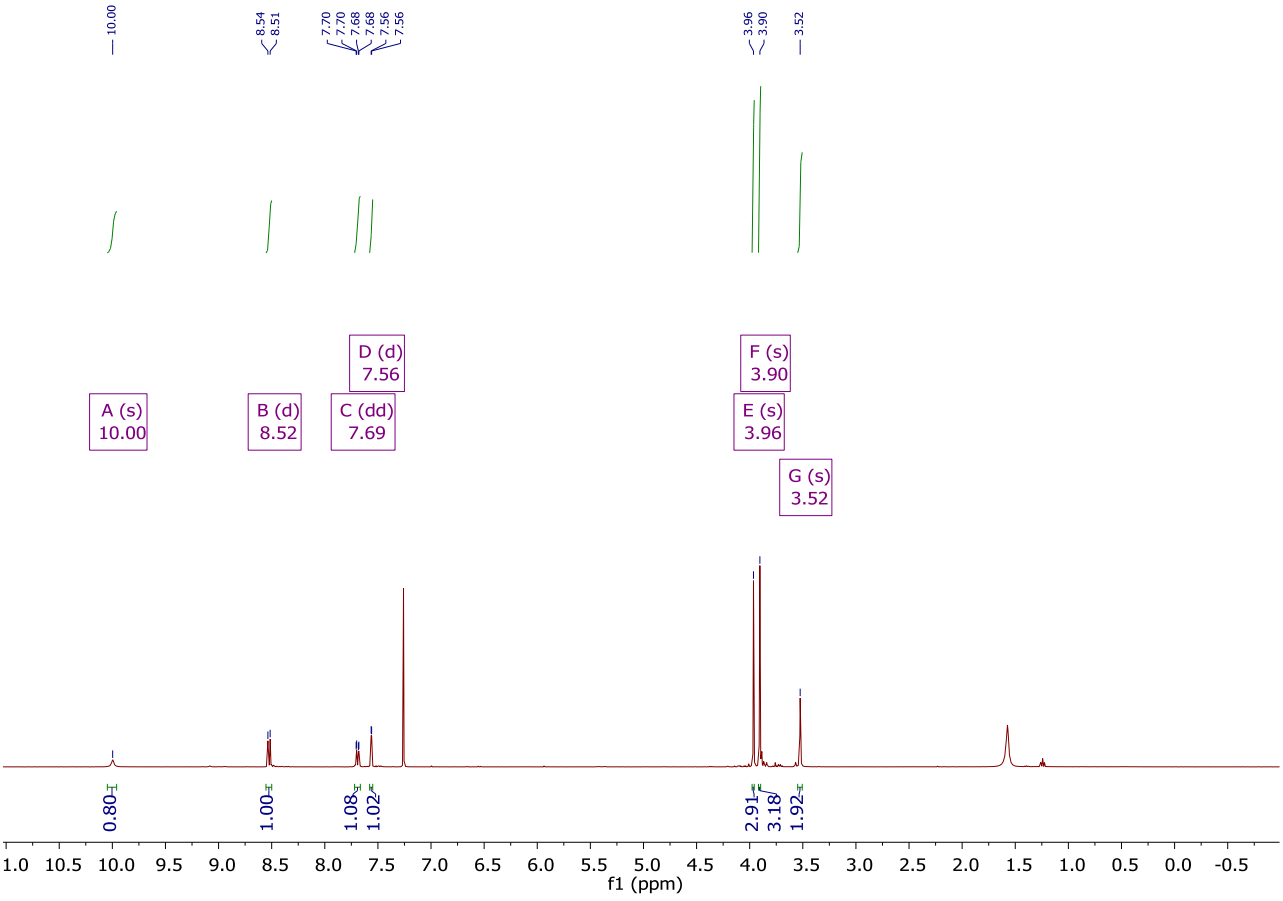

^{13}C-NMR:

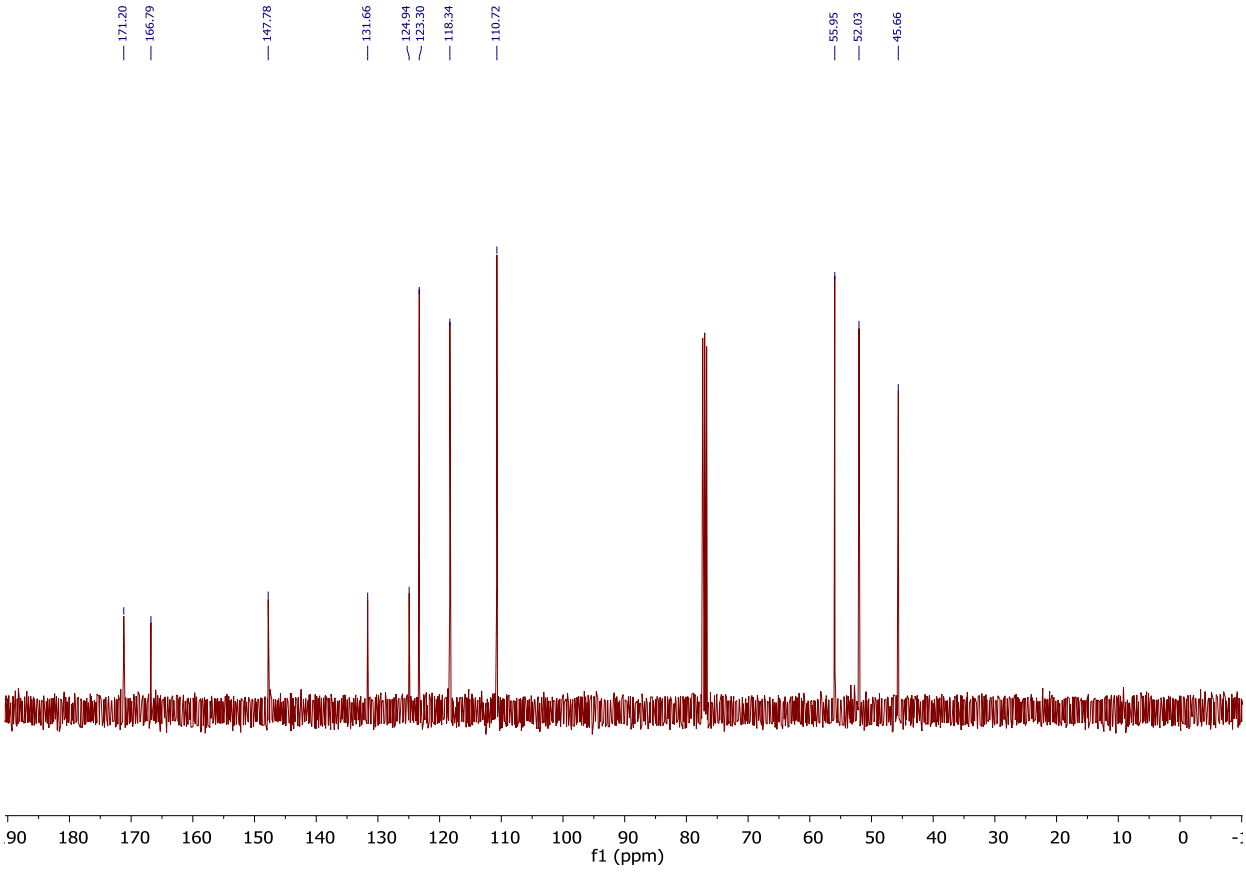

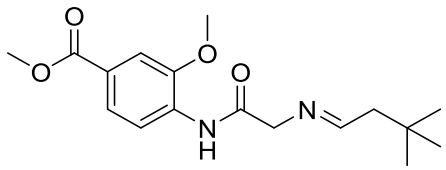

methyl (E)-4-(2-((3,3-dimethylbutylidene)amino)acetamido)-3-methoxybenzoate (**3**)

To a solution **2** (300 mg, 1.26 mmol) in dry DCM (10 mL) under N_2 atmosphere was added 3,3-dimethylbutanal (174 mL, 1.38 mmol) and $MgSO_4$ (227 mg, 1.89 mmol) and the resulting suspension was stirred for 16h at RT. Subsequently, the suspension was filtered and the residue washed with DCM (10 mL). Evaporation of the filtrate yielded the crude product (302 mg, 67%) as a yellow oil which was used in the next step without further purification.

^{1}H NMR (400 MHz, $CDCl_3$): δ 9.45 (s, 1H), 8.52 (d, *J* = 8.5 Hz, 1H), 7.84 (tt, *J* = 5.6, 1.5 Hz, 1H), 7.69 (dd, *J* = 8.4, 1.8 Hz, 1H), 7.55 (s, 1H), 4.21 (s, 2H), 3.93 (s, 3H), 3.90 (s, 3H), 2.27 (d, *J* = 5.7 Hz, 2H), 1.03 (s, 9H). Data in accordance with literature.[7]

^{1}H-NMR:

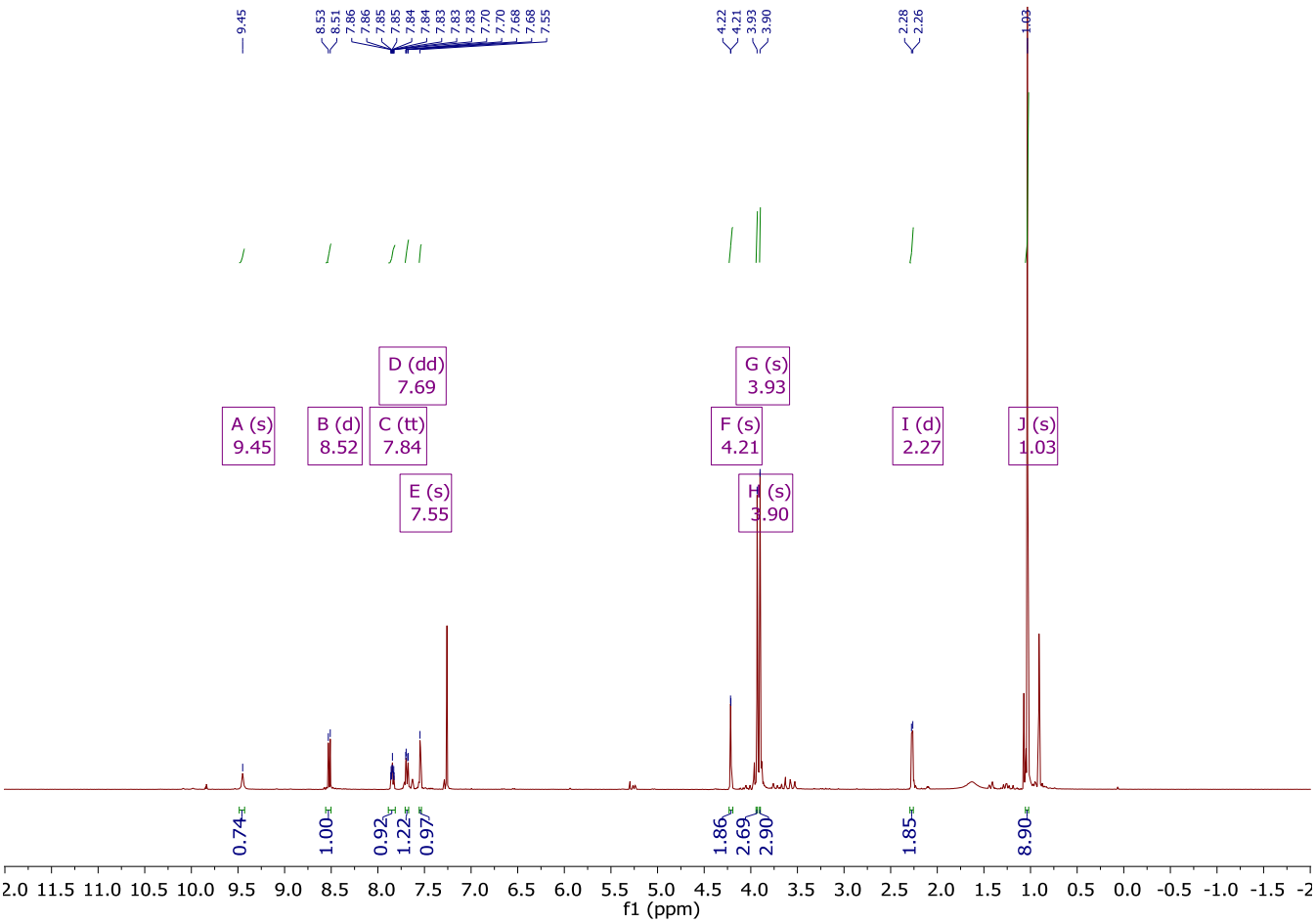

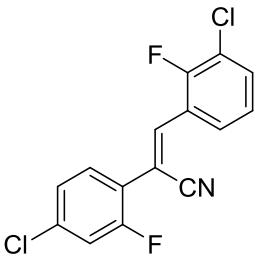

(Z)-3-(3-chloro-2-fluorophenyl)-2-(4-chloro-2-fluorophenyl)acrylonitrile (**4**)

To a solution of 3-chloro-2-fluorobenzaldehyde (468 mg, 2.95 mmol) and 2-(4-chloro-2-fluorophenyl)acetonitrile (500 mg, 2.95 mmol) in EtOH (10 mL) and H_2O (40 µL) was added NaOEt (10.0 mg, 0.15 mmol) and subsequently the reaction mixture was stirred for 3h at RT. The resulting suspension was filtered and the precipitate was washed with EtOH. Evaporation *in vacuo* yielded the crude product which was dissolved in DCM (10 mL) and washed with brine (3 x 20 mL) and dried ($MgSO_4$). Evaporation of the volatiles yielded the pure product (650 mg, 71%) as a white solid.

^{1}H NMR (400 MHz, DMSO-d_6): δ 7.97 (td, *J* = 6.8, 1.4 Hz, 1H), 7.88 (s, 1H), 7.77 (ddd, *J* = 8.6, 7.4, 1.6 Hz, 1H), 7.72 (t, *J* = 8.5 Hz, 1H), 7.66 (dd, *J* = 11.0, 2.1 Hz, 1H), 7.47 (ddd, *J* = 8.4, 2.1, 0.8 Hz, 1H), 7.42 (td, *J* = 8.0, 1.1 Hz, 1H). In accordance with literature.[6]

^{19}F NMR (376 MHz, DMSO-d_6): δ -111.41 (dd, *J* = 11.1, 8.6 Hz), -115.42 (t, *J* = 7.0 Hz).

^{1}H-NMR:

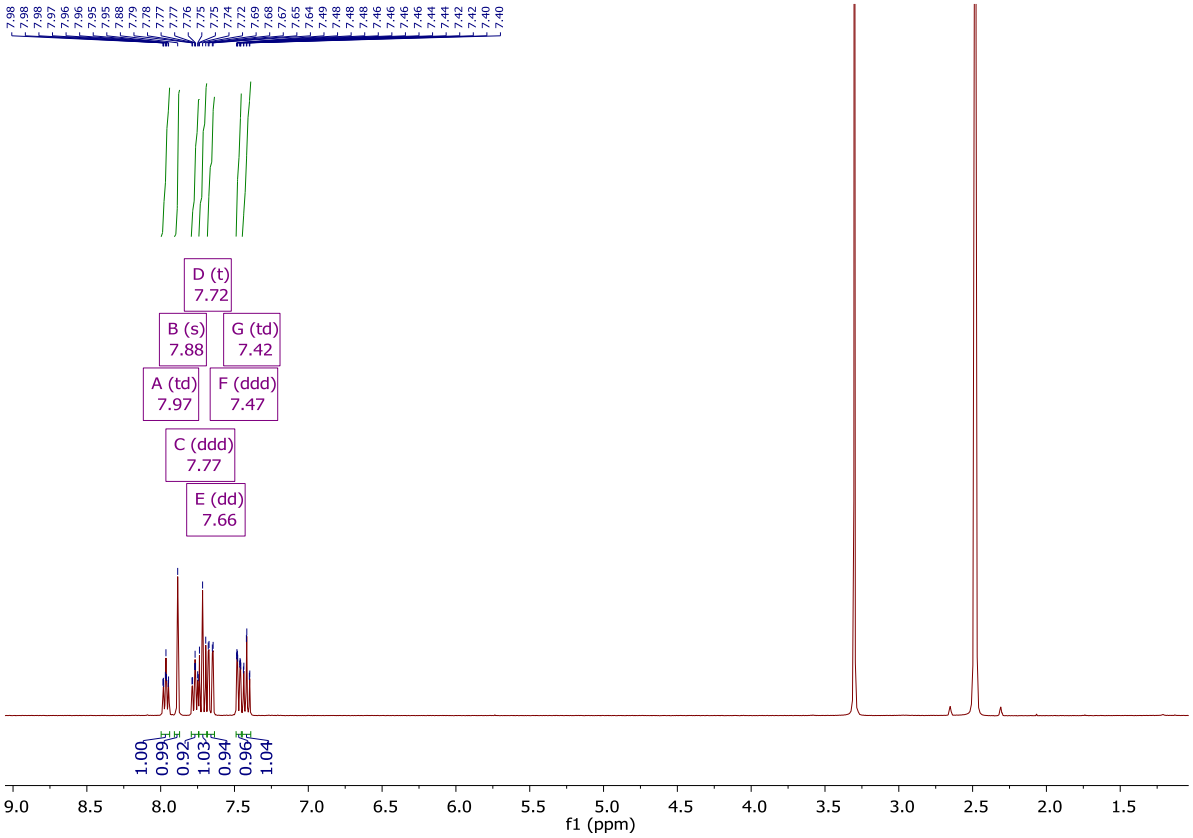

^{19}F-NMR:

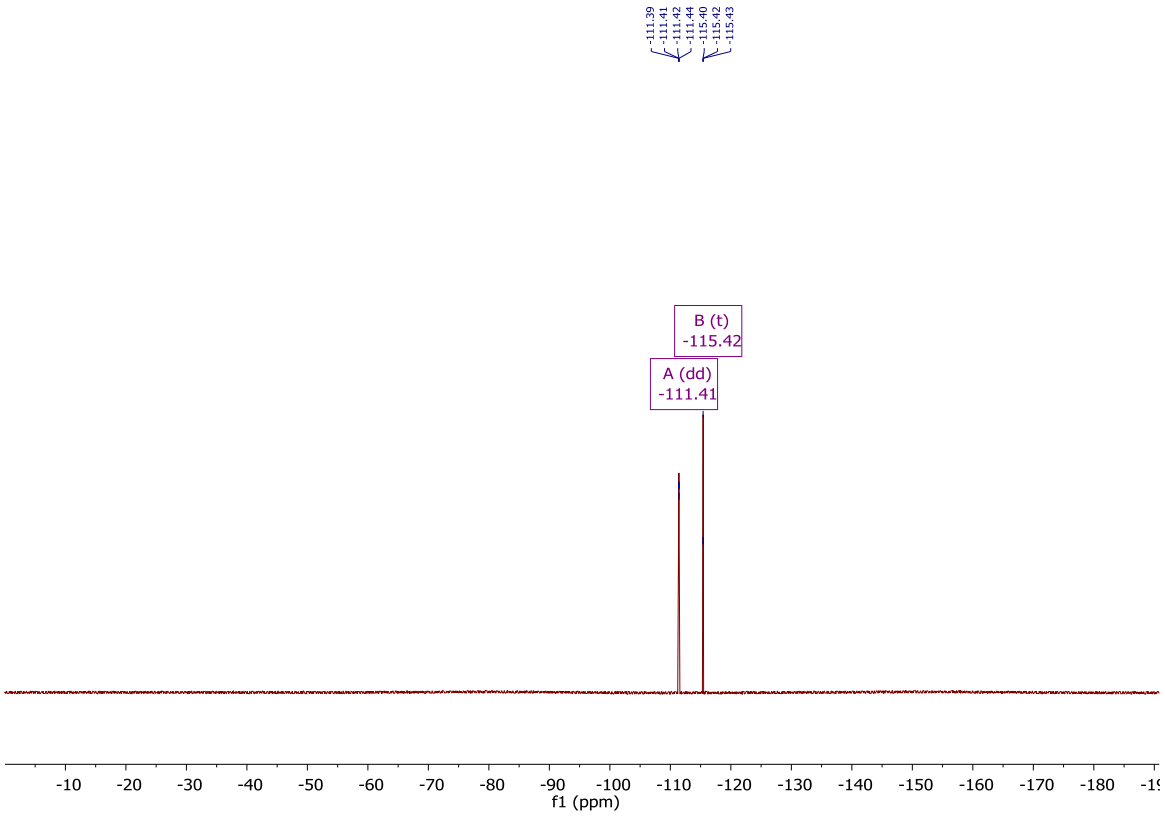

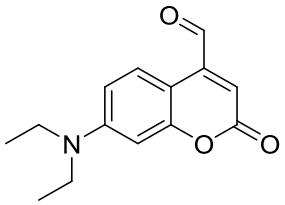

7-(diethylamino)-2-oxo-2H-chromene-4-carbaldehyde (**5**)

A solution of 7-(diethylamino)-4-methyl-coumarin (500 mg, 2.16 mmol) and SeO_2 (480 mg, 4.32 mmol) in *p*-xylene (20 mL) was heated to 150 °C for 16h under N_2 atmosphere in the dark. Subsequently, the solution was filtered while hot and concentrated *in vacuo*. Purification by column chromatography (DCM) yielded the pure product (223 mg, 42%) as an orange viscous oil.

^{1}H NMR (400 MHz, $CDCl_3$): δ 10.03 (s, 1H), 8.31 (d, *J* = 9.2 Hz, 1H), 6.63 (dd, *J* = 9.2, 2.6 Hz, 1H), 6.53 (d, *J* = 2.6 Hz, 1H), 6.45 (s, 1H), 3.43 (q, *J* = 7.1 Hz, 4H), 1.22 (t, *J* = 7.1 Hz, 6H). Data in accordance with literature.[8]

^{1}H-NMR:

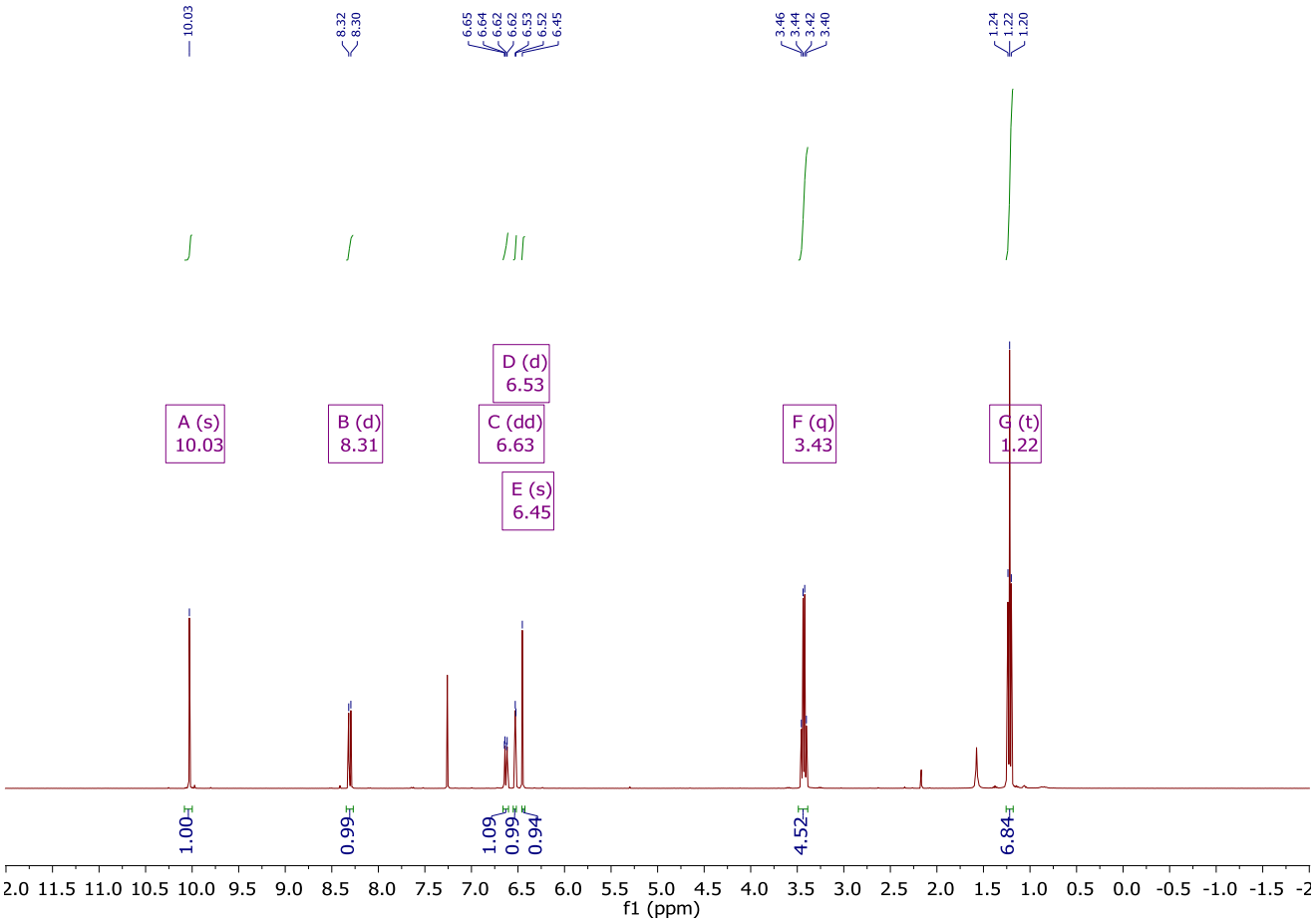

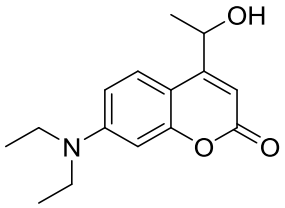

7-(diethylamino)-4-(1-hydroxyethyl)-2H-chromen-2-one (**6**)

To a solution of **5** (220 mg, 0.89 mmol) in dry THF (8 mL) under N_2 atmosphere at -78 °C was slowly added MeMgBr in THF (3M, 534 µL, 1.60 mmol) and the reaction mixture was stirred for 2.5h at -78 °C in the dark. Subsequently, sat. aq. NH_4Cl was added (10 mL) and the mixture was allowed to warm to RT. The organic layer was separated and the aqueous layer extracted with EtOAc (2 x 10 mL). The combined organic layers were washed with brine (20 mL), dried and evaporated *in vacuo* to yield the crude product. Column chromatography (pentane: acetone, 3:1) yielded the pure product (125 mg, 54%) as an orange solid.

^{1}H NMR (400 MHz, $CDCl_3$): δ 7.42 (d, *J* = 9.0 Hz, 1H), 6.57 (dd, *J* = 9.0, 2.7 Hz, 1H), 6.52 (d, *J* = 2.6 Hz, 1H), 6.27 (d, *J* = 0.9 Hz, 1H), 5.22 – 5.09 (m, 1H), 3.41 (q, *J* = 7.1 Hz, 4H), 1.57 (d, *J* = 4.7 Hz, 3H), 1.21 (t, *J* = 7.1 Hz, 6H). Data in accordance with literature.[9]

^{1}H-NMR:

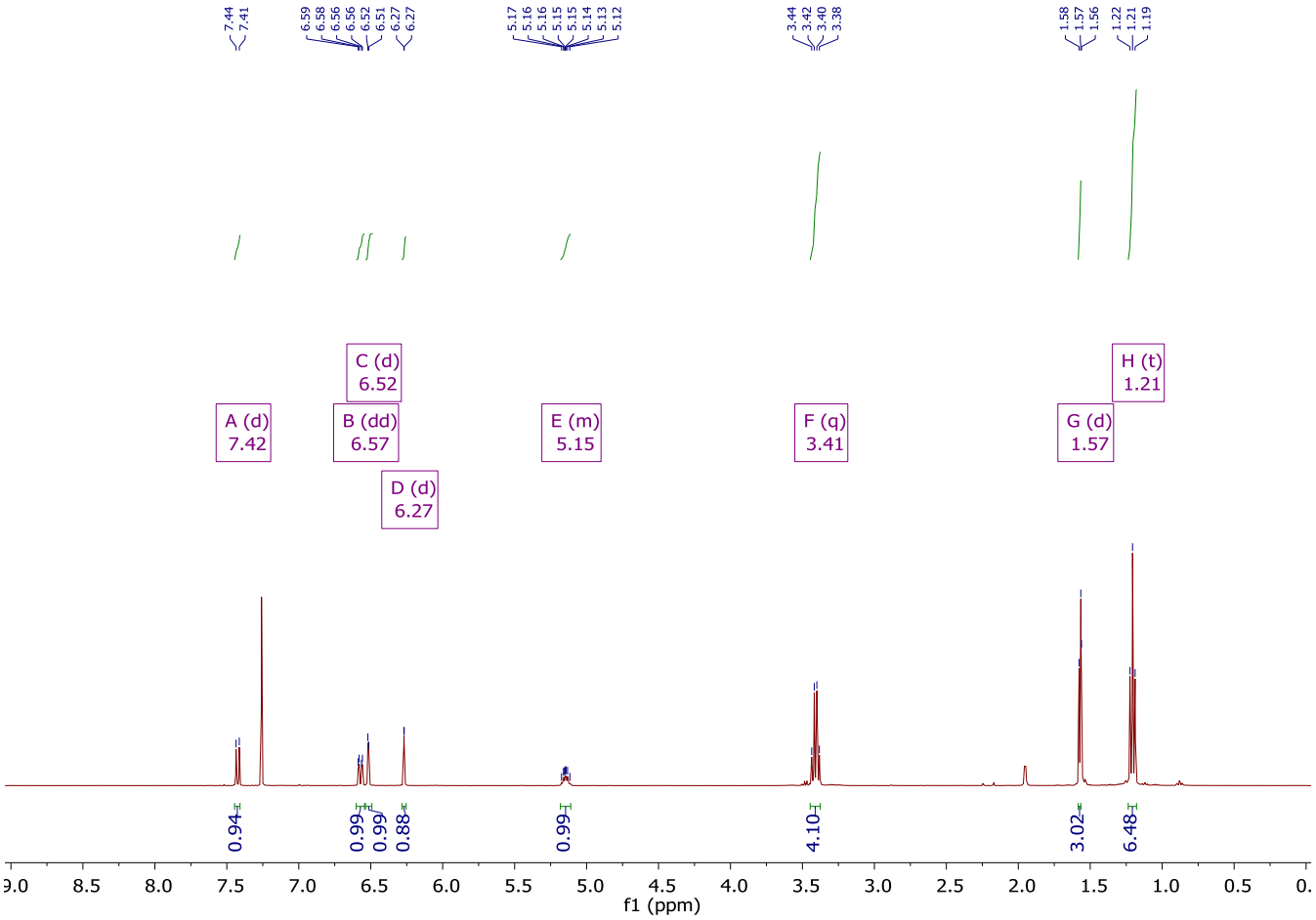

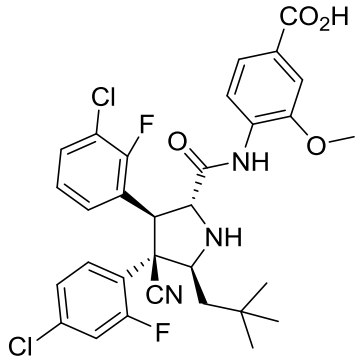

4-((2R,3S,4R,5S)-3-(3-chloro-2-fluorophenyl)-4-(4-chloro-2-fluorophenyl)-4-cyano-5-neopentylpyrrolidine-2-carboxamido)-3-methoxybenzoic acid (**7**)

A solution of CuOAc (0.56 mg, 4.58 μmol) and R-BINAP (3.0 mg, 4.81 μmol) in THF (5 mL) was slowly added to a suspension of **3** (302 mg, 0.95 mmol) and **4** (279 mg, 0.90 mmol) in THF (5 ml) under N_2 atmosphere at RT. Subsequently, Et_3N (123 mL, 0.88 mmol) was added and the resulting mixture was stirred for 5h at RT. Next, THF (10 mL) was added and the resulting solution was washed twice with aq. NH_4OAc (10 mL, 10% w/w) and brine (10 mL). Subsequently, the organic layers were evaporated and the crude product was dissolved in THF (7 mL) and EtOH (3 mL). 2.5M aq. NaOH (1 mL) was added and the mixture was stirred for 18h at RT. The solution was acidified with AcOH to pH = 6.0 and the volatiles were partially evaporated (2 mL). After addition of H_2O (10 mL) the precipitate was filtered to give the crude product (493 mg, 89%) as an off-white solid. Subsequent enantioenrichment and purification was performed by crystallization. The crude product (493 mg) was dissolved in THF (6 mL) and heated to 65 °C. Subsequently EtOAc (2 mL) was added and the resulting solution was heated for 15 min after which it was cooled to RT and filtered. The residue was washed with EtOAc (5 mL) and the filtrate evaporated *in vacuo*. The crude product was dissolved in MeCN (7 mL) and heated to 80 °C after which it was slowly cooled to 10 °C. The precipitate was filtered yielding the pure product (118 mg, 21%) as a white solid.

^{1}H NMR (400 MHz, DMSO-d_6): δ 12.85 (s, 1H), 10.45 (s, 1H), 8.35 (d, *J* = 8.8 Hz, 1H), 7.71 (t, *J* = 7.3 Hz, 1H), 7.62 – 7.50 (m, 4H), 7.44 – 7.28 (m, 3H), 4.66 – 4.52 (m, 2H), 4.37 (s, 1H), 3.91-3.85 (m, 4H), 1.63 (dd, *J* = 14.2, 9.9 Hz, 1H), 1.25 (d, *J* = 14.2 Hz, 1H), 0.96 (s, 9H). Data in accordance with literature.[6]

HR-MS (ESI, [M+H]$^+$): Calcd. for $C_{31}H_{31}Cl_2F_2N_3O4$: 616.1576; Found: 616.1575

^{1}H-NMR:

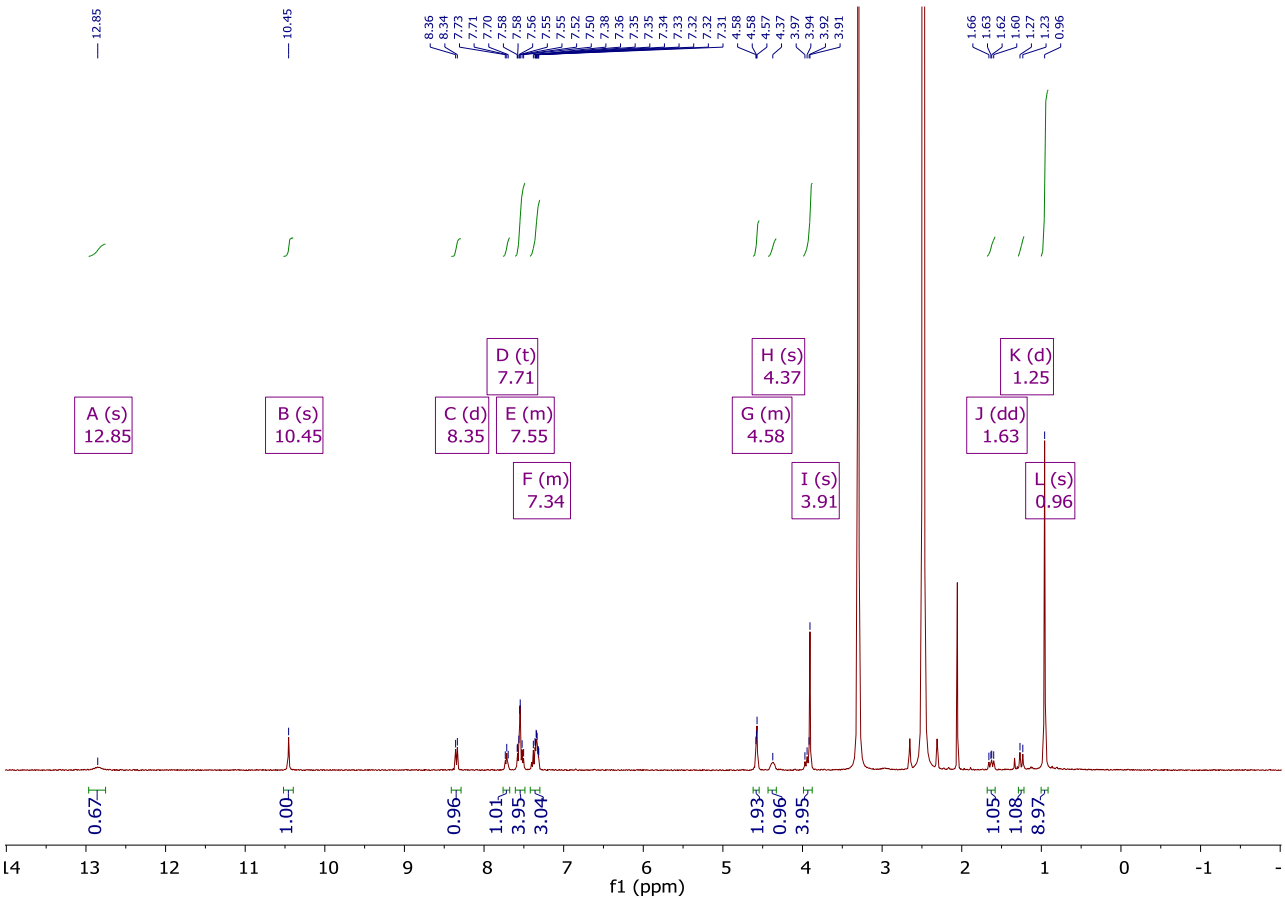
A (s) 12.85
B (s) 10.45
C (d) 8.35
D (t) 7.71
E (m) 7.55
F (m) 7.34
G (m) 4.58
H (s) 4.37
I (s) 3.91
J (dd) 1.63
K (d) 1.25
L (s) 0.96
f1 (ppm)

HR-MS:

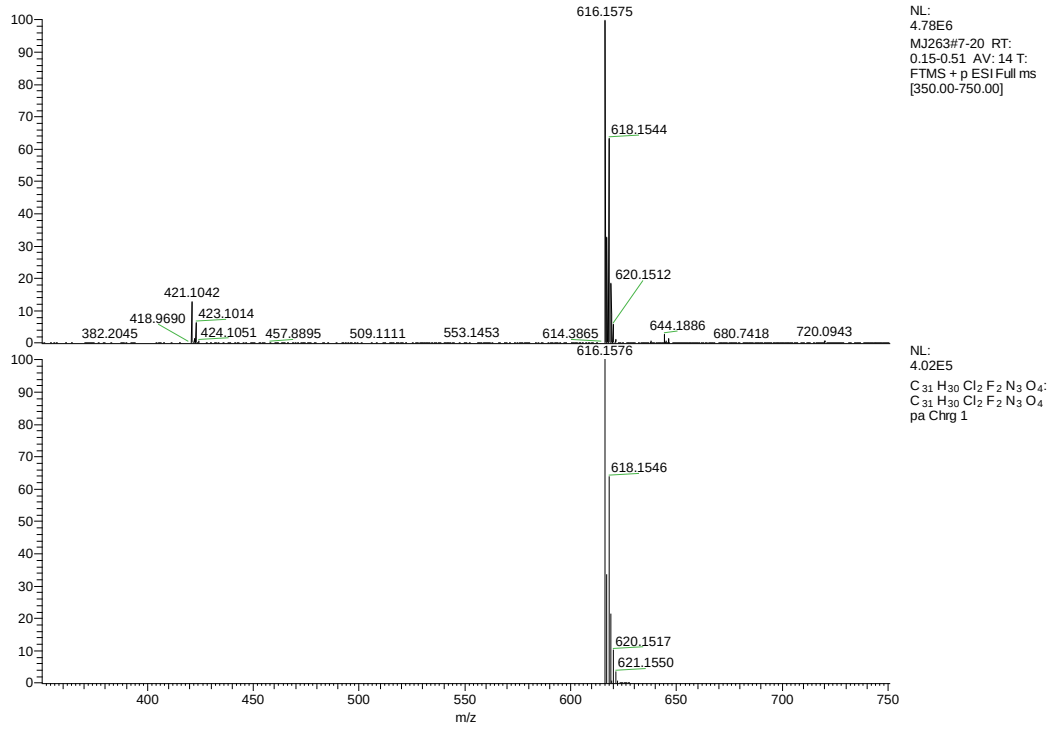
616.1575
618.1544
620.1512
421.1042
423.1014
418.9690
424.1051
382.2045
457.8895
509.1111
553.1453
614.3865
644.1886
680.7418
720.0943
NL:
4.78E6
MJ263#7-20 RT:
0.15-0.51 AV: 14 T:
FTMS + p ESI Full ms
[350.00-750.00]
616.1576
618.1546
620.1517
621.1550
NL:
4.02E5
C31 H30 Cl2 F2 N3 O4:
C31 H30 Cl2 F2 N3 O4
pa Chrg 1
m/z

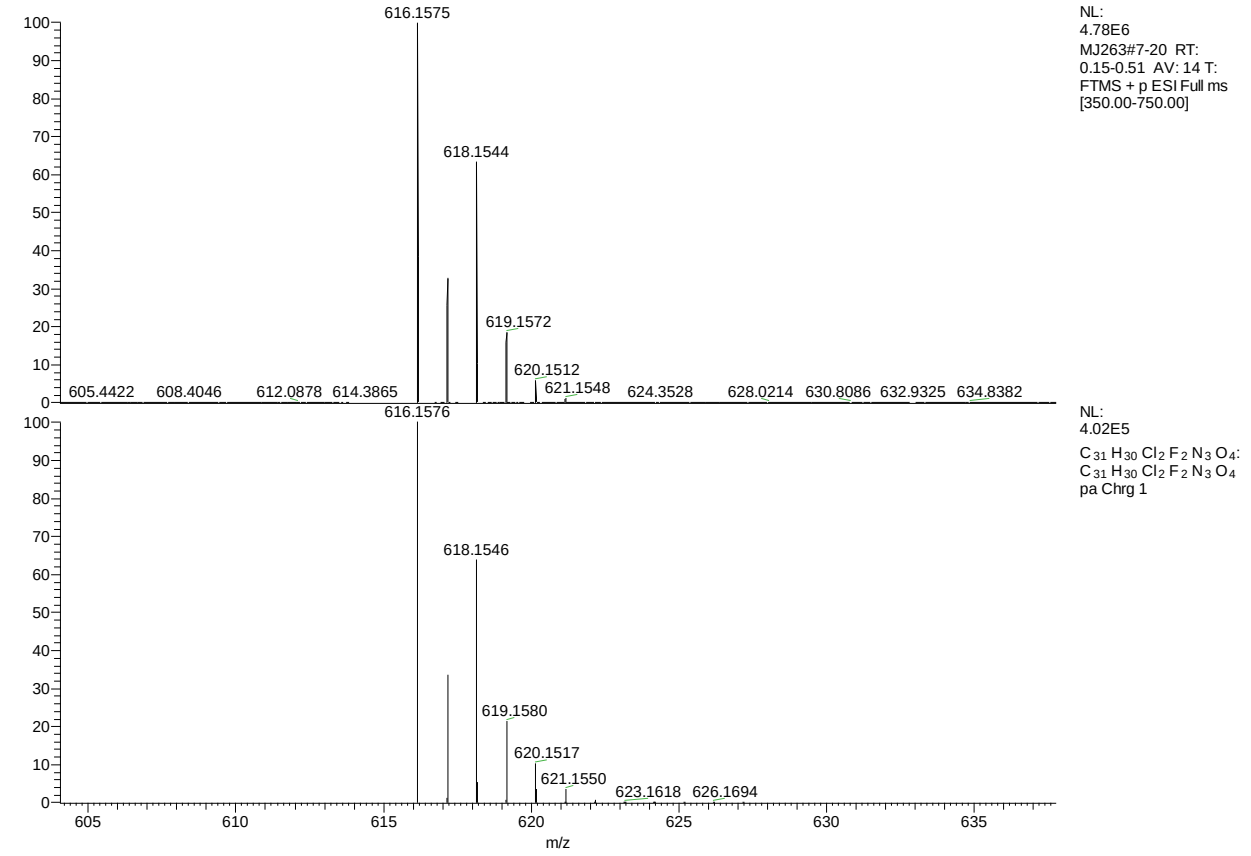

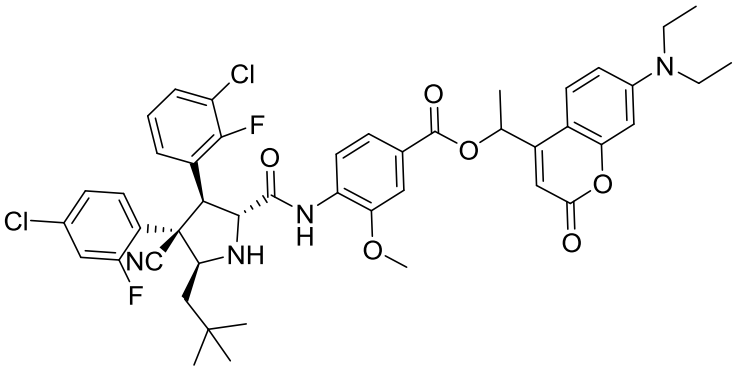

1-(7-(diethylamino)-2-oxo-2H-chromen-4-yl)ethyl 4-((2R,3S,4R,5S)-3-(3-chloro-2-fluorophenyl)-4-(4-chloro-2-fluorophenyl)-4-cyano-5-neopentylpyrrolidine-2-carboxamido)-3-methoxybenzoate (**PPG-idasanutlin (8)**)

To a solution of **7** (100 mg, 0.16 mmol) and **6** (47 mg, 0.18 mmol) in dry DCM (3 mL) under N_2 atmosphere was added EDC.HCl (37 mg, 0.19 mmol) and DMAP (5 mg, 0.04 mmol) at 0 °C. Subsequently, the reaction mixture was allowed to warm to RT and stirred for 16h. Subsequently, DCM (10 mL) was added and the resulting solution was washed with 0.5M aq. HCl (3 x 10 mL), sat. aq. $NaHCO_3$ (2 x 10 mL) and brine (10 mL) and dried ($MgSO_4$). All the volatiles were evaporated to yield the crude product (135 mg). Column chromatography (pentane:ethyl acetate, 3:1) yielded the pure product (55 mg, 40%) as a bright yellow solid.

^{1}H NMR (400 MHz, DMSO-d_6): δ 10.51 (s, 1H), 8.42 (d, *J* = 7.0 Hz, 1H), 7.74 – 7.66 (m, 3H), 7.62 (s, 1H), 7.59 – 7.49 (m, 2H), 7.42 – 7.31 (m, 3H), 6.72 (d, *J* = 9.3 Hz, 1H), 6.54 (s, 1H), 6.24 (q, *J* = 6.6 Hz, 1H), 6.02 (s, 1H), 4.64 – 4.55 (m, 2H), 4.44 – 4.36 (m, 1H), 3.99 – 3.90 (m, 4H), 3.42 (q, *J* = 6.7 Hz, 4H), 1.65 (d, *J* = 6.8 Hz, 3H), 1.63 – 1.60 (m, 1H), 1.25 (d, *J* = 14.3 Hz, 1H), 1.11 (t, *J* = 6.9 Hz, 6H), 0.96 (s, 9H).

^{13}C NMR (151 MHz, DMSO-d_6): δ 171.8, 164.7, 161.3, 160.8, 159.1, 156.8, 156.7, 156.6, 155.2, 150.9, 148.1, 135.2, 132.1, 131.4, 130.5, 129.1, 126.3, 126.1, 125.7, 124.5, 123.5, 120.0, 119.6, 118.1, 117.7, 111.5, 109.4, 105.3, 103.8, 97.5, 68.8, 65.1, 63.7, 56.3, 50.6, 44.4, 44.3, 30.5, 29.9, 21.2, 12.7.

^{19}F NMR (376 MHz, DMSO-d_6): δ -108.31 (dd, *J* = 12.2, 8.8 Hz), -120.95.

HR-MS (ESI, [M+H]$^+$): Calcd. for $C_{46}H_{47}Cl_2F_2N_4O_6$: 859.2835; Found: 859.2841

^{1}H-NMR:

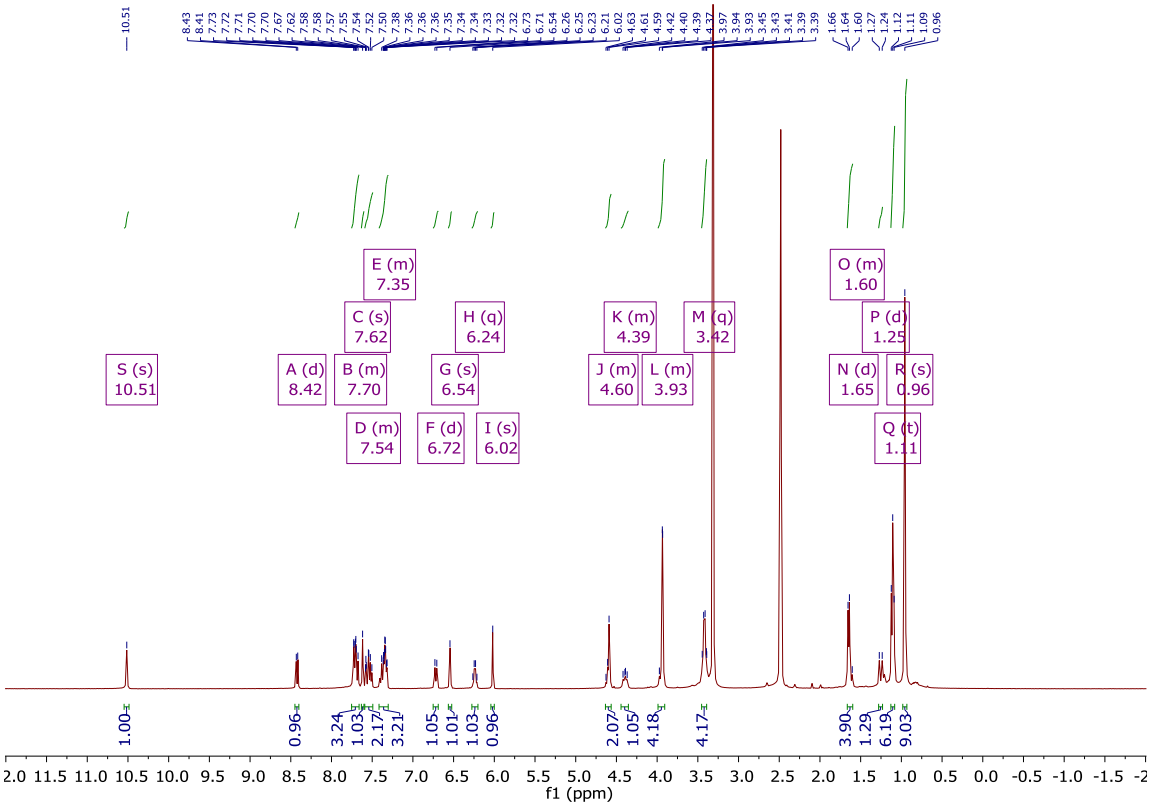

^{13}C-NMR

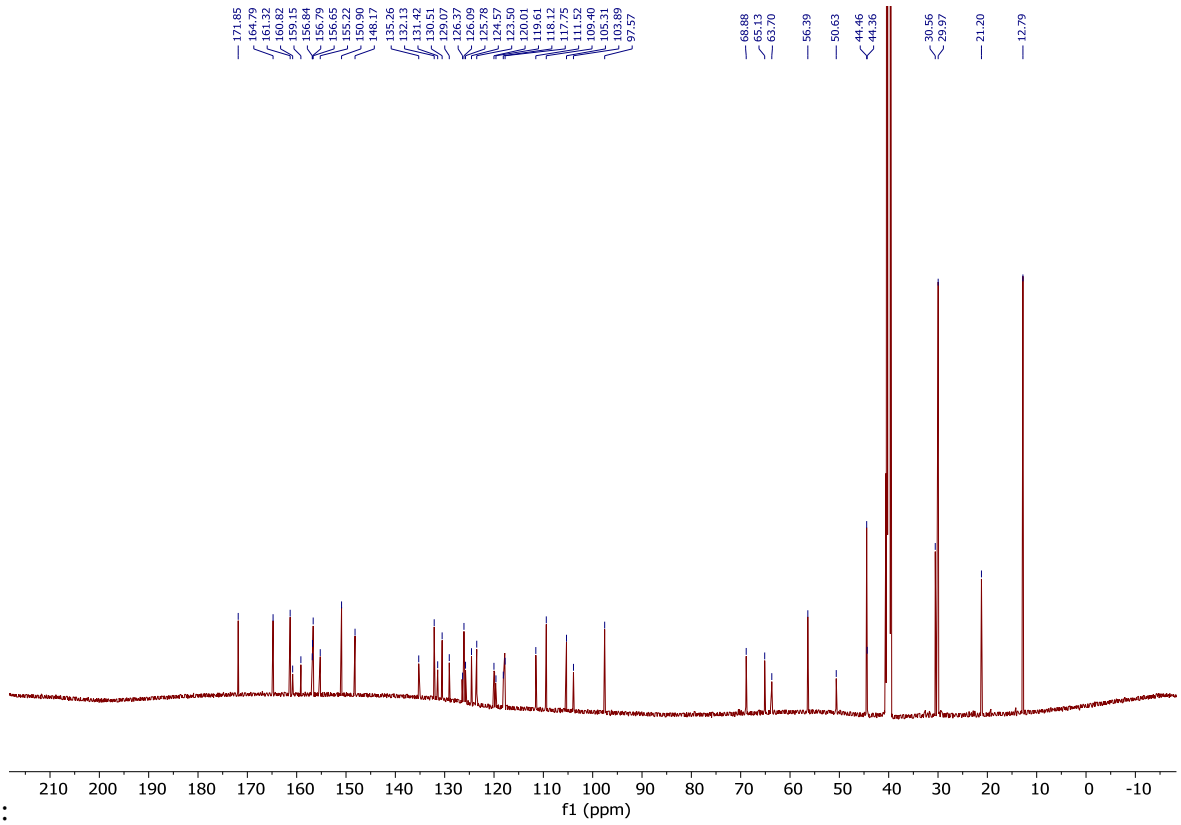

:

^{19}F-NMR:

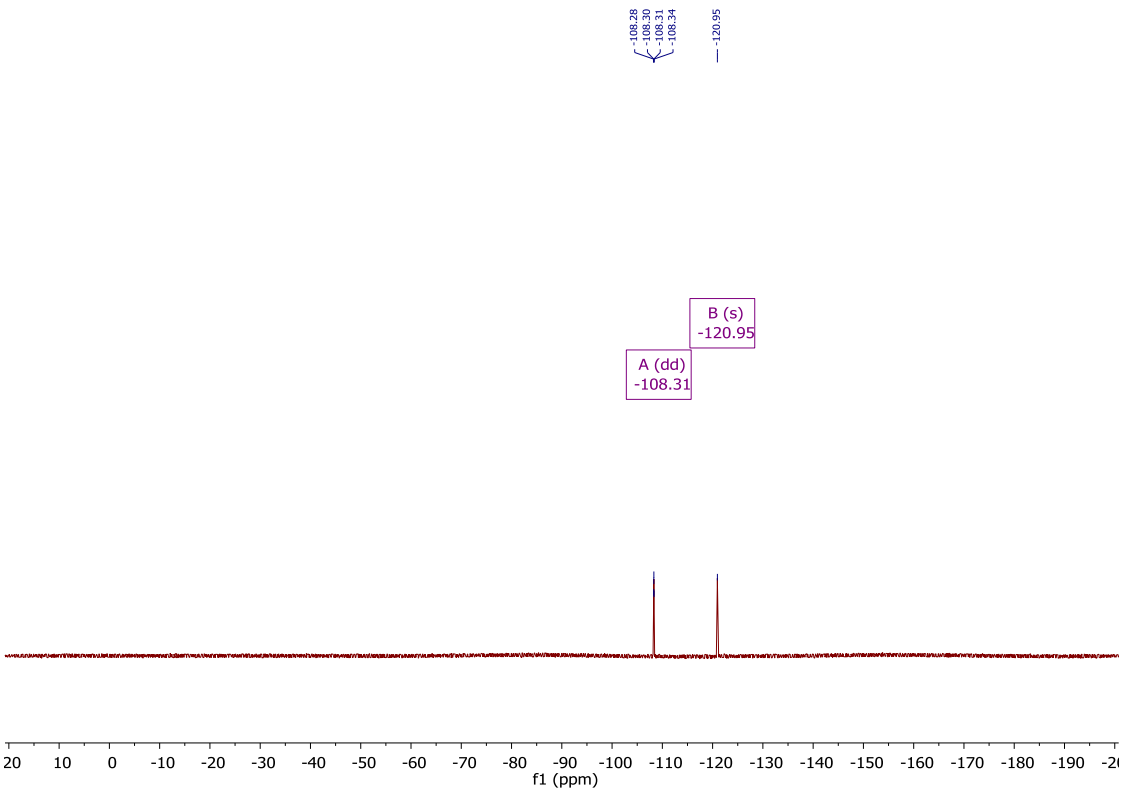

HSQC

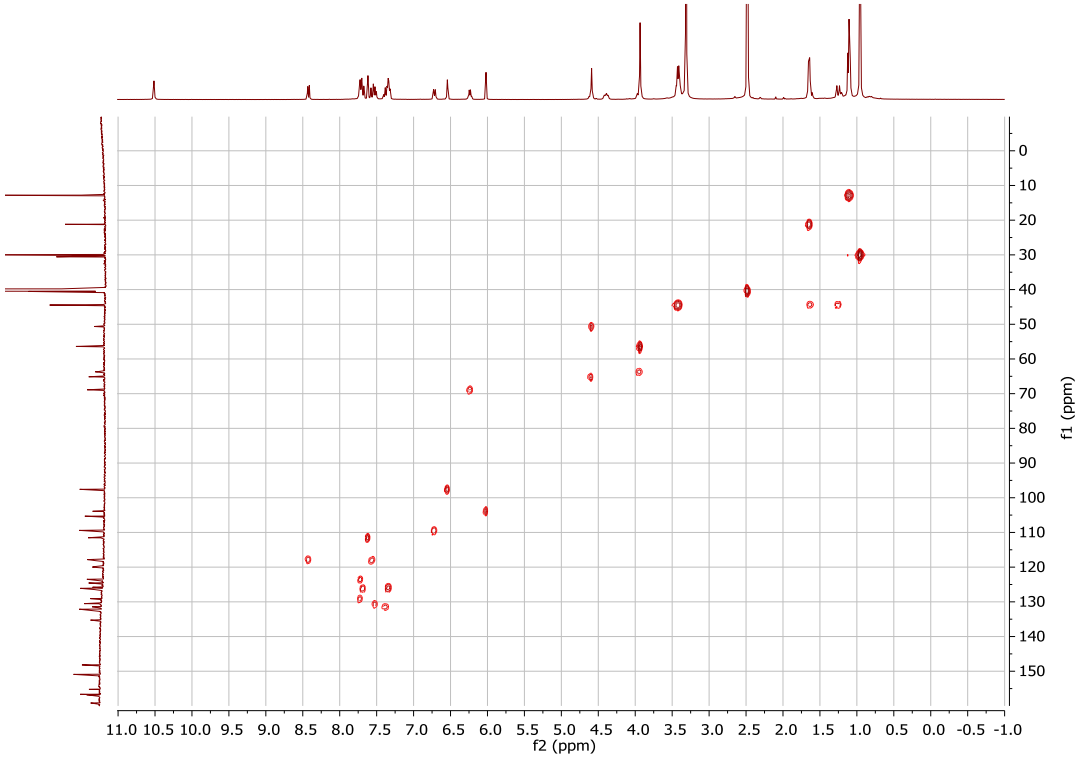

HSQC:

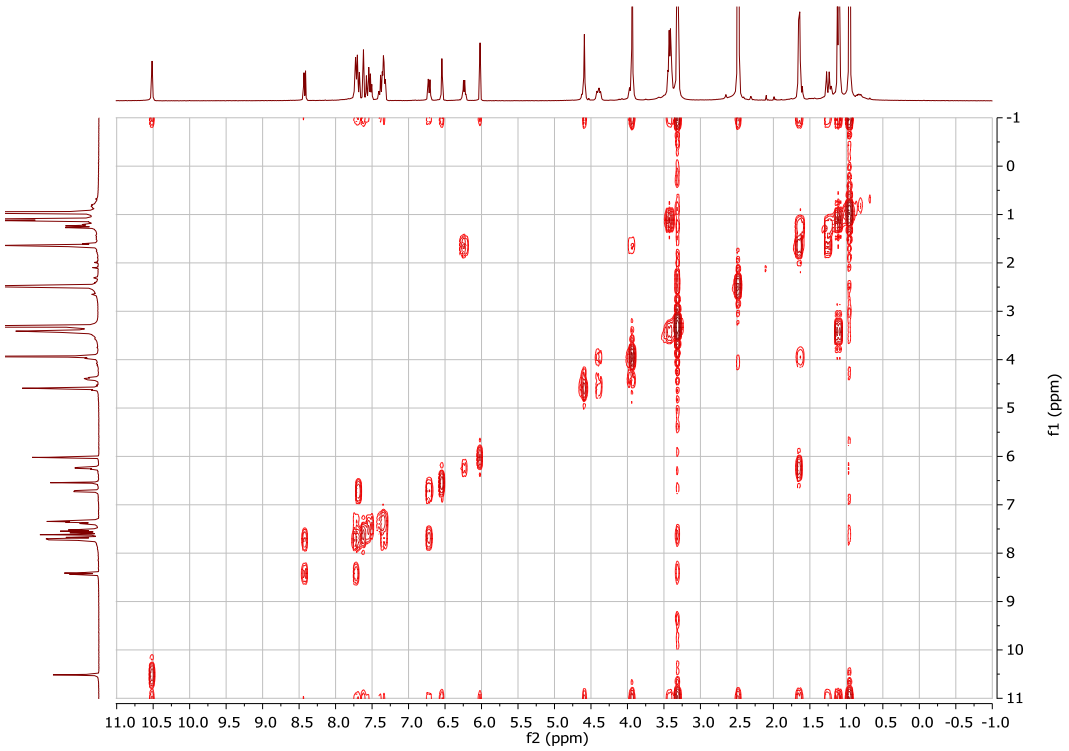

HR-MS:

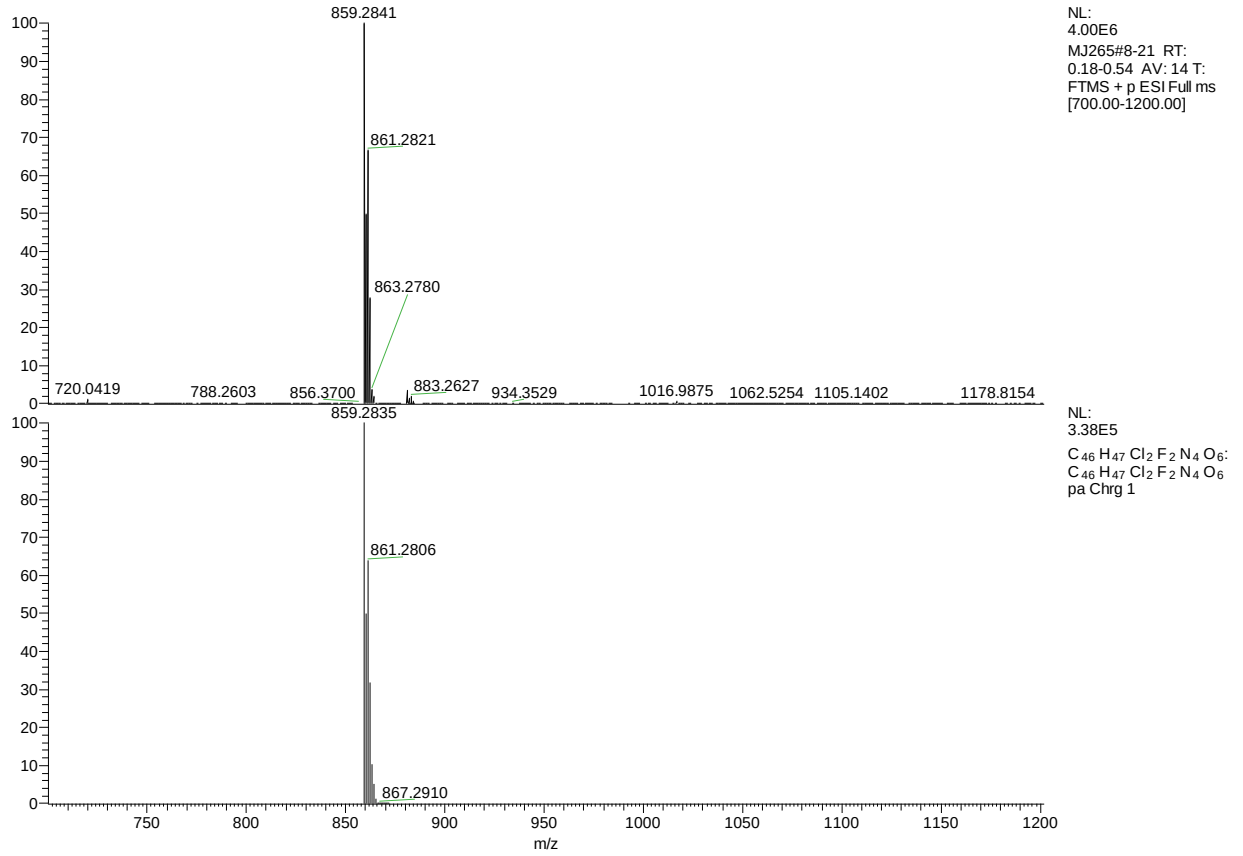
859.2841
861.2821
863.2780
720.0419
788.2603
856.3700
883.2627
934.3529
1016.9875
1062.5254
1105.1402
1178.8154
859.2835
NL:
4.00E6
MJ265#8-21 RT:
0.18-0.54 AV: 14 T:
FTMS + p ESI Full ms
[700.00-1200.00]
NL:
3.38E5
C46 H47 Cl2 F2 N4 O6:
C46 H47 Cl2 F2 N4 O6
pa Chrg 1
861.2806
867.2910
m/z

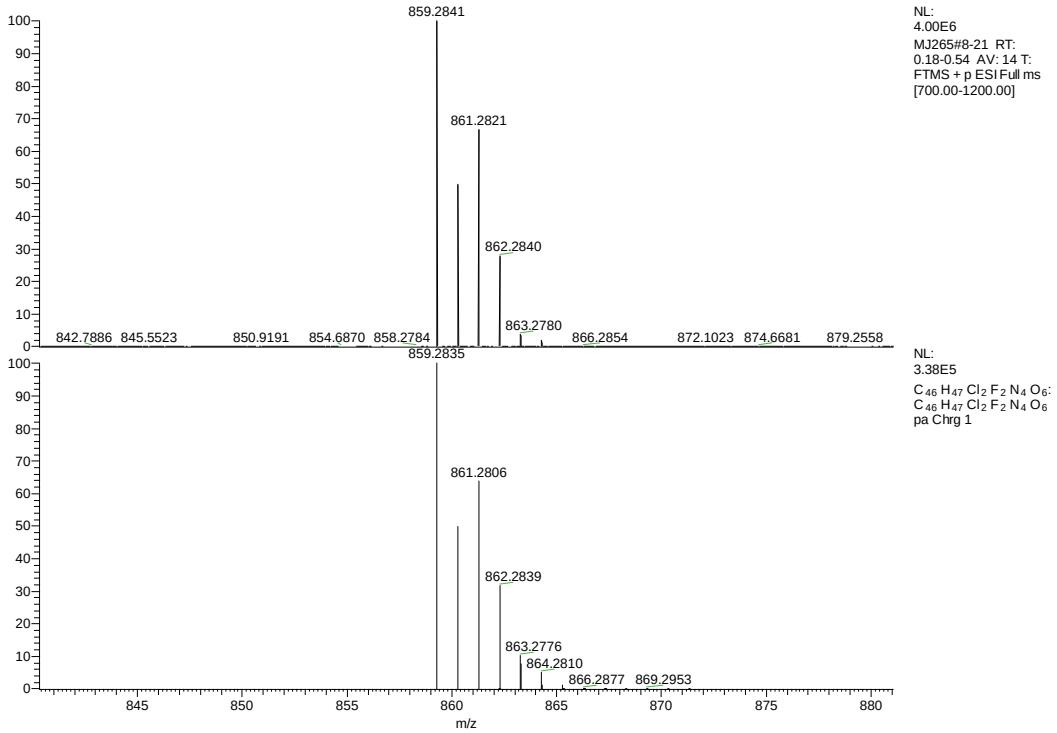
859.2841
861.2821
862.2840
863.2780
842.7886
845.5523
850.9191
854.6870
858.2784
866.2854
872.1023
874.6681
879.2558
859.2835
NL:
4.00E6
MJ265#8-21 RT:
0.18-0.54 AV: 14 T:
FTMS + p ESI Full ms
[700.00-1200.00]
NL:
3.38E5
C46 H47 Cl2 F2 N4 O6:
C46 H47 Cl2 F2 N4 O6
pa Chrg 1
861.2806
862.2839
863.2776
864.2810
866.2877
869.2953
m/z

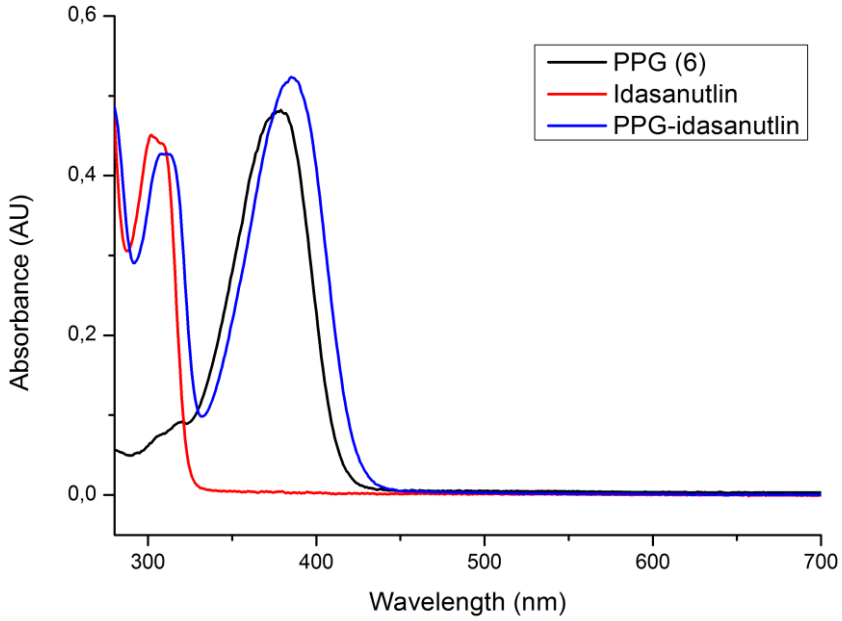

Figure S5: Absorbance spectra of PPG-idasanutlin (8), PPG (6) and idasanutlin (7) in mixed buffer (TRIS, Bis-TRIS, MES, NaOAc, 25 mM each) pH = 7.0, (20 μM).

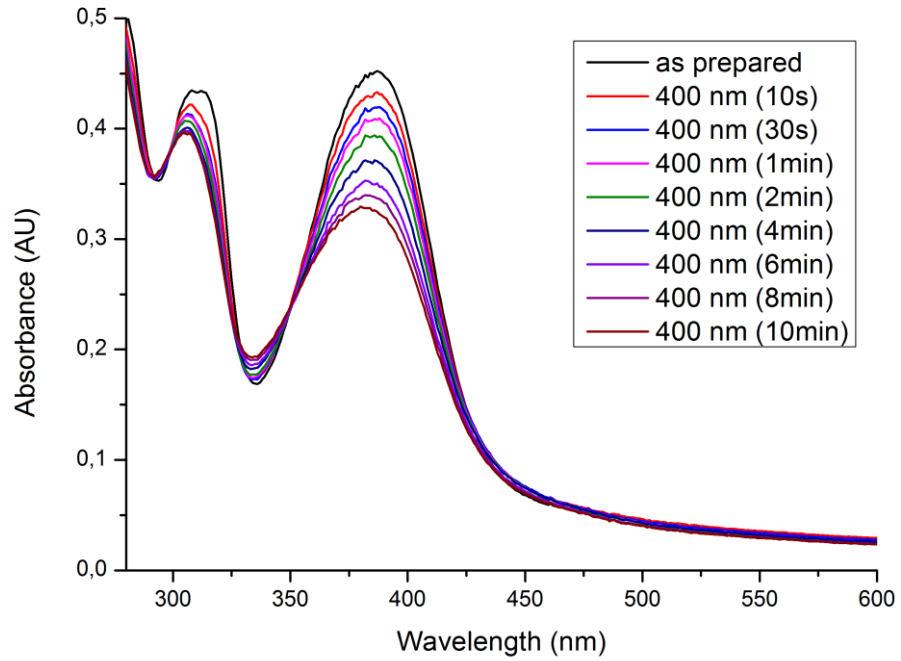

Figure S6: Photocleavage of PPG-idasanutlin (8) in mixed buffer (TRIS, Bis-TRIS, MES, NaOAc, 25 mM each) with 1% DMSO at pH = 7.0 (20 μM).

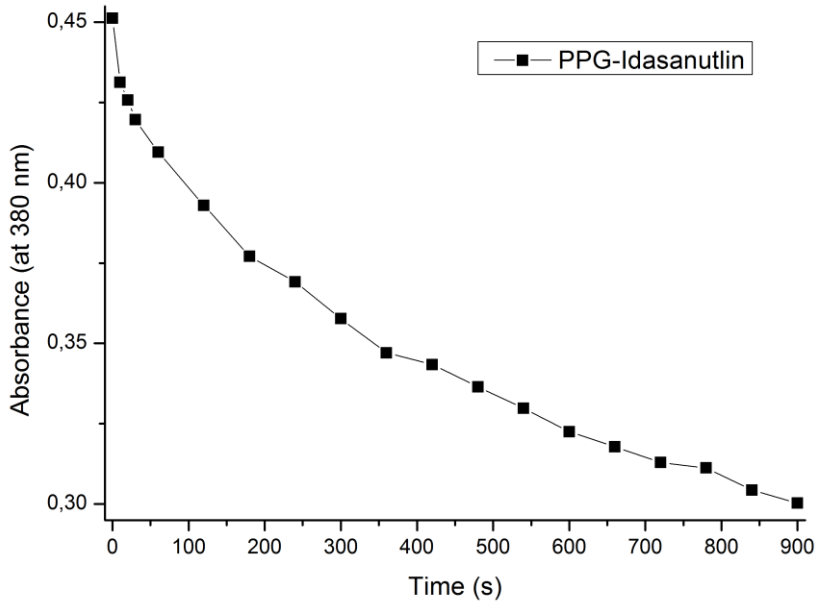

Figure S7: Photocleavage of PPG-idasanutlin (8) in mixed buffer (TRIS, Bis-TRIS, MES, NaOAc, 25 mM each) pH = 7.0 (20 μM) measured at 380 nm over time.

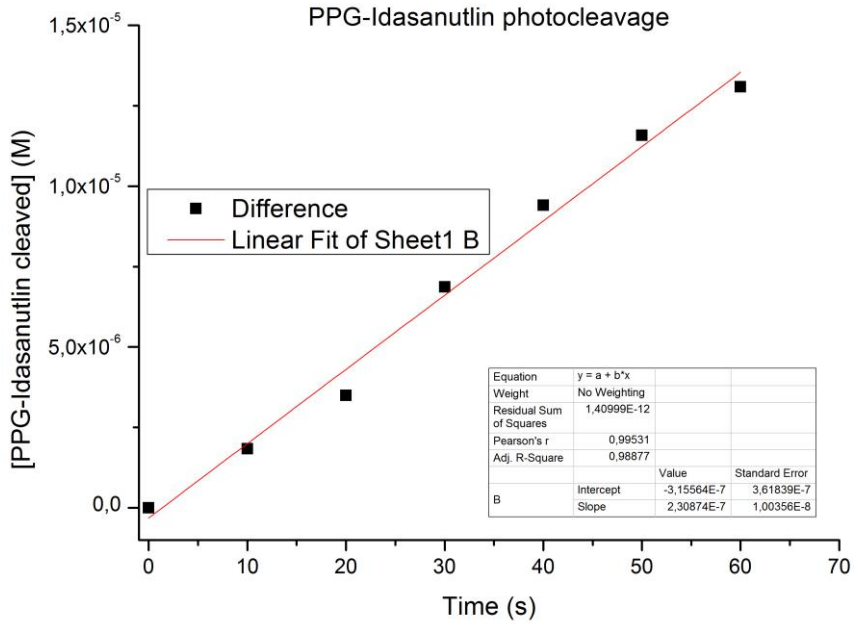

Figure S8: Photocleavage quantum yield of PPG-idasanutlin (8) in DMSO. Seven independent data point are taken from which a linear fit was obtained giving the slope and standard error. From this the quantum yield has been determined to be 0.11% (Std E: 0.0047%).

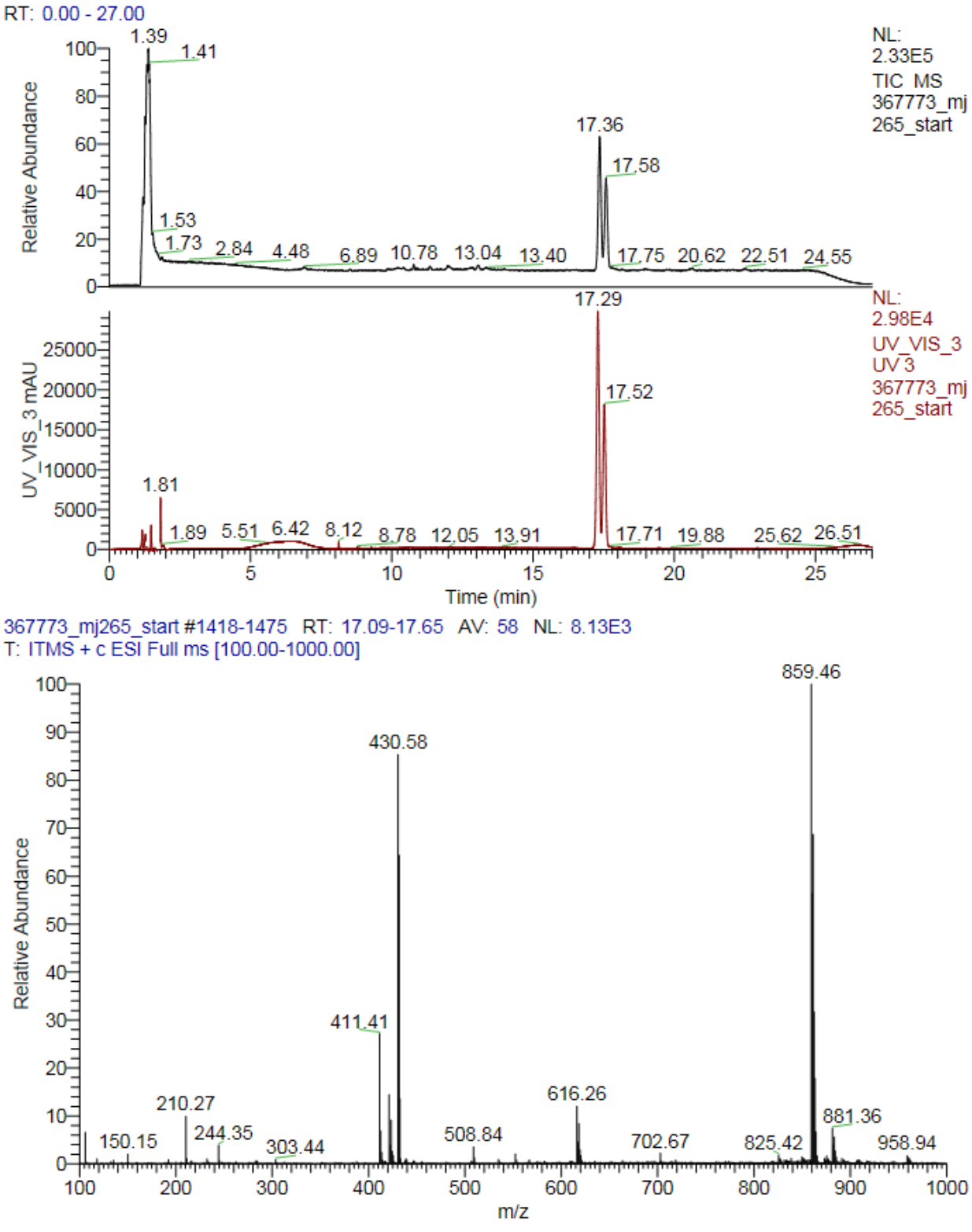

Figure S9: UPLC-MS trace of PPG-idasanutlin (RT: 17.36, 17.58) showing two epimers with the mass according to the expected structure.

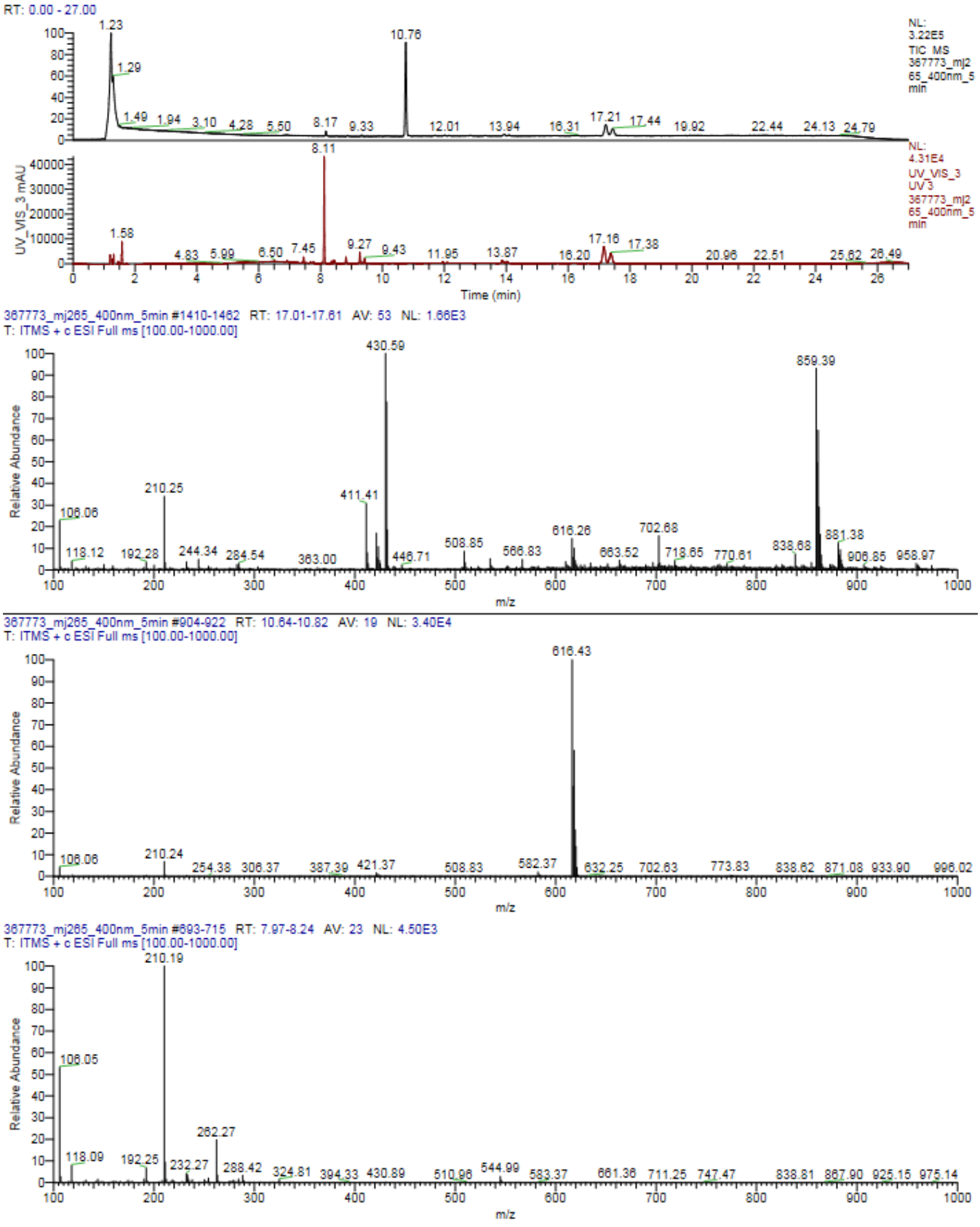

Figure S10: UPLC-MS trace after 5 min irradiation of PPG-idasanutlin (RT: 17.21) with 400 nm light (buffer (TRIS, Bis-TRIS, MES, NaOAc, 25 mM each), 20 µM, pH= 7.0), showing the release of compound 7 (RT: 10.76) and photoproduct 6 (RT: 8.11).

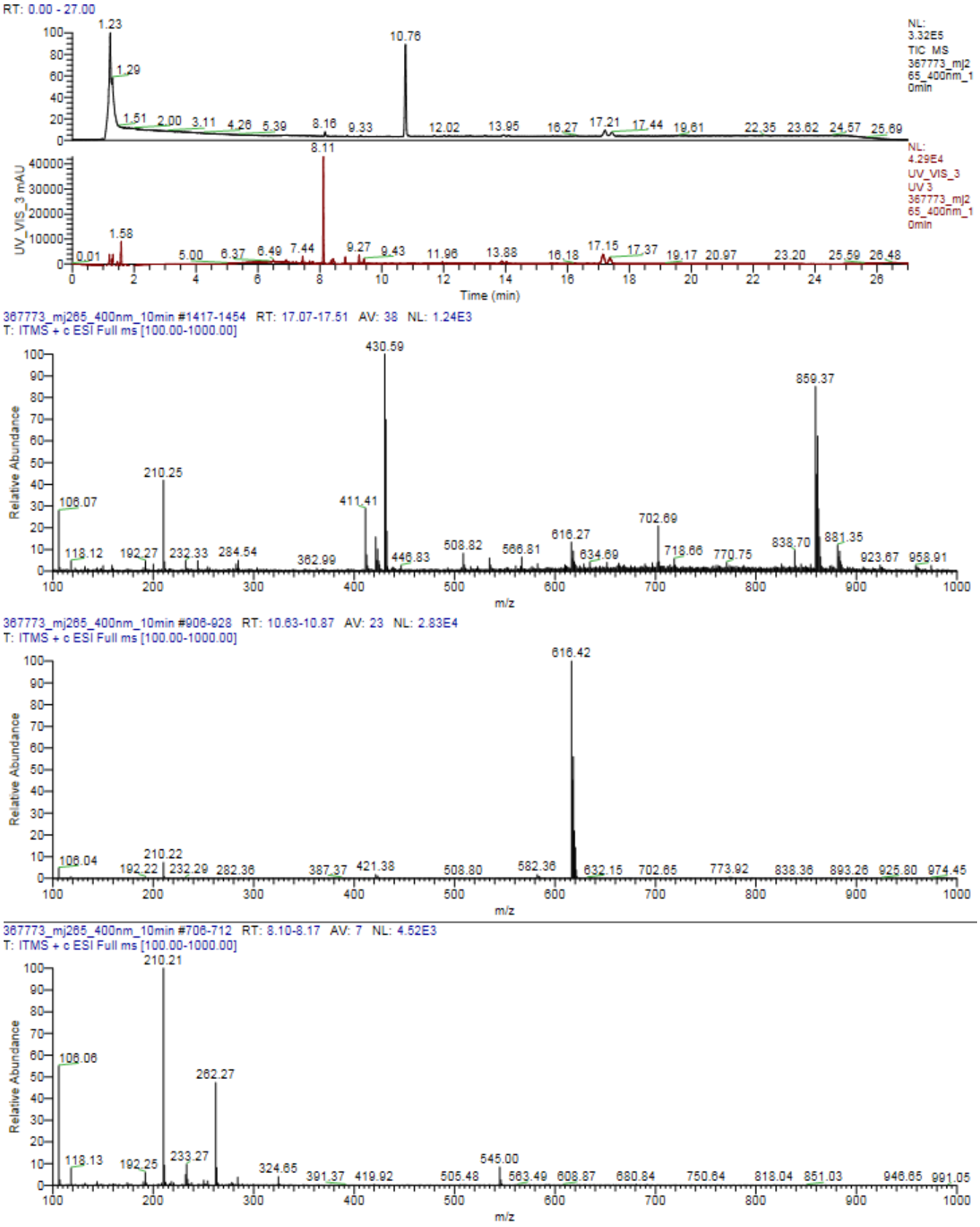

Figure S11: UPLC-MS trace after 10 min irradiation of PPG-idasanutlin (RT: 17.21) with with 400 nm light (buffer, (TRIS, Bis-TRIS, MES, NaOAc, 25 mM each), 20 μM, pH= 7.0), showing the release of compound 7 (RT: 10.76) and photoproduct 6 (RT: 8.11).

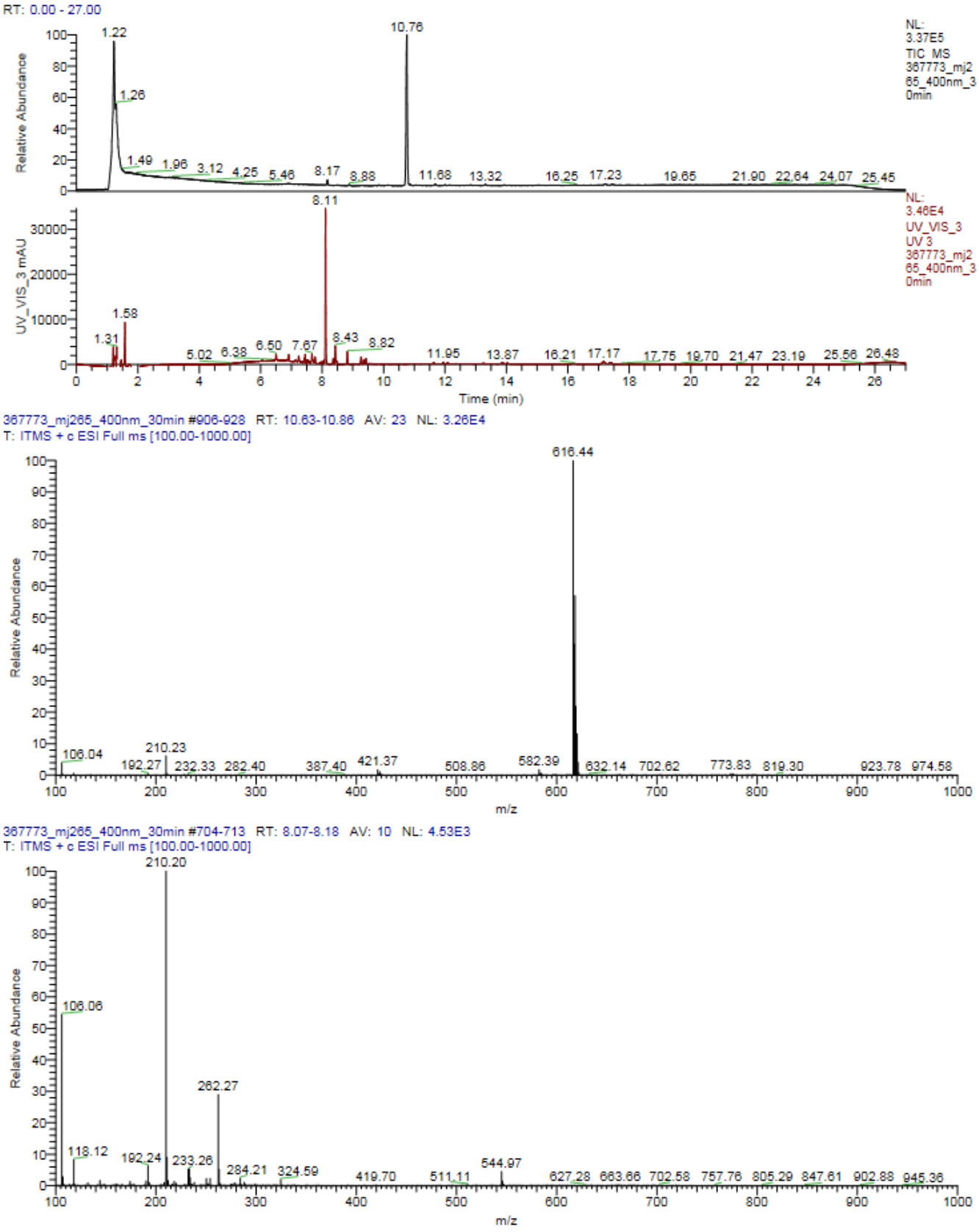

Figure S12: UPLC-MS trace after 30 min irradiation of PPG-idasanutlin with with 400 nm light (buffer, (TRIS, Bis-TRIS, MES, NaOAc, 25 mM each), 20 µM, pH= 7.0), showing the release of compound 7 (RT: 10.76) and photoproduct 6 (RT: 8.11) and no trace of PPG-idasanutlin (RT: 17.21) remaining.

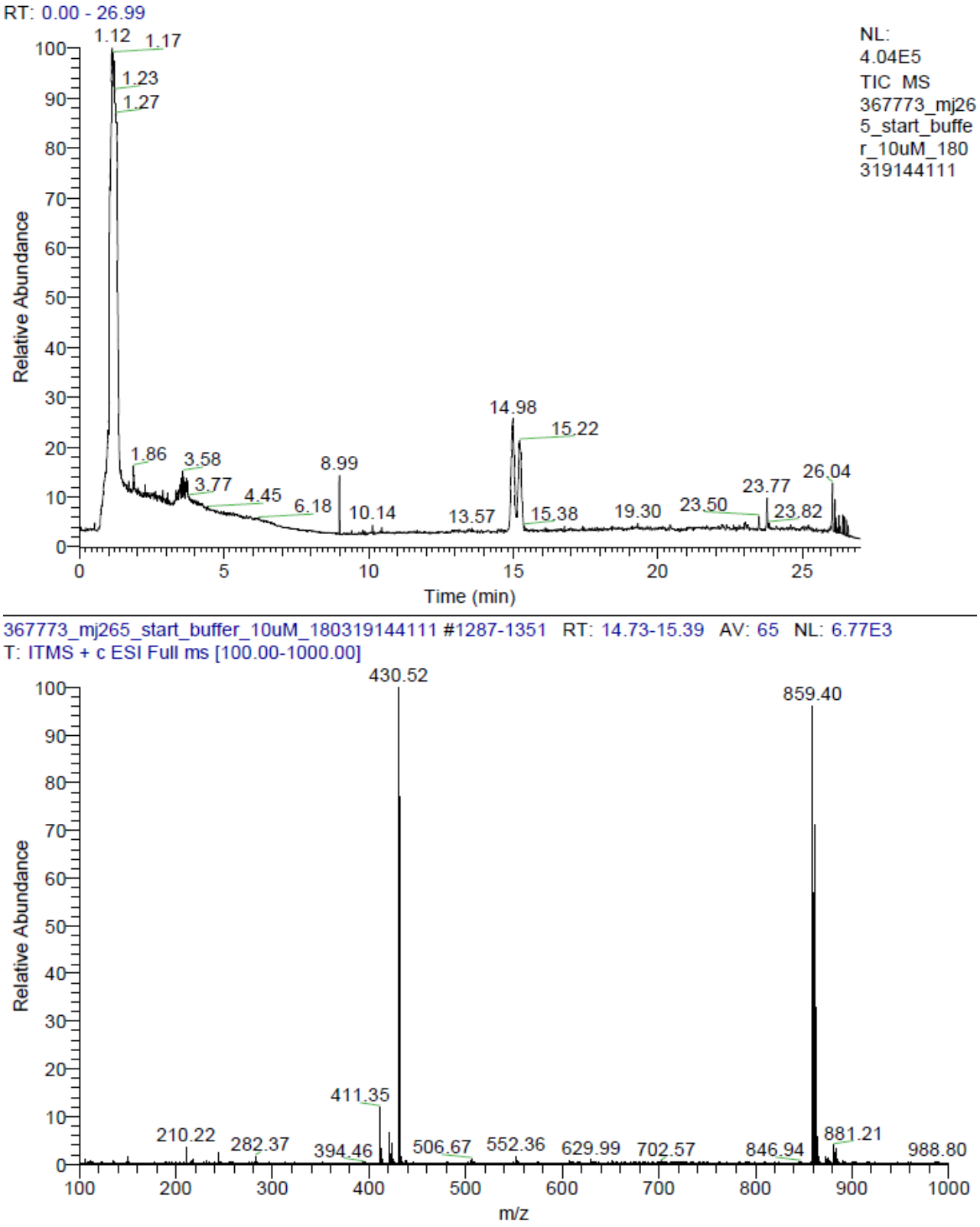

Figure S13: PPG-idasanutlin (RT: 14.98-15.22)in buffer (TRIS, Bis-TRIS, MES, NaOAc, 25 mM each), (10 μM) at starting point.

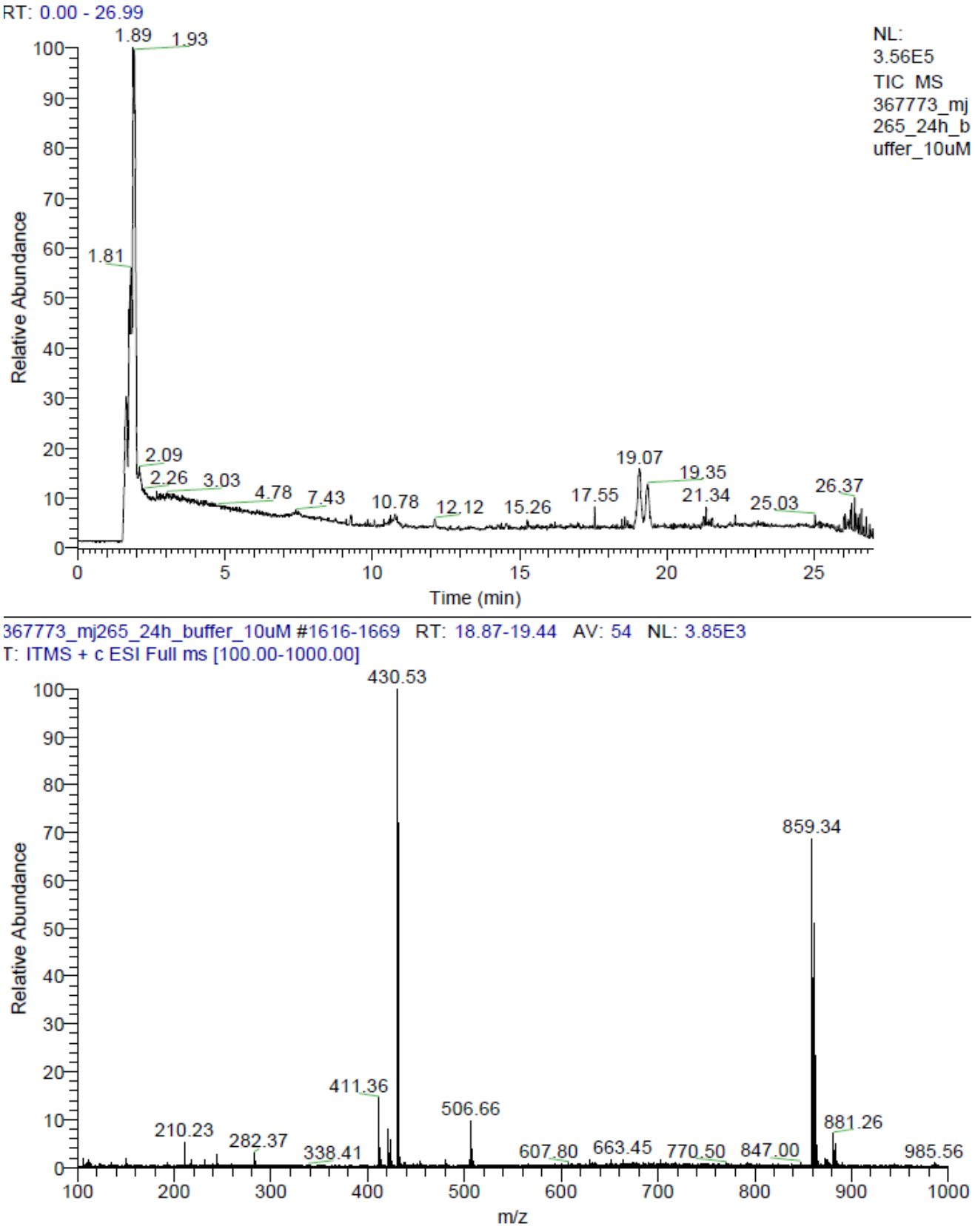

Figure S14: PPG-idasanutlin (RT: 19.07-19.35) after 24h in buffer (TRIS, Bis-TRIS, MES, NaOAc, 25 mM each), (10 µM) at RT, no hydrolysis (evolution of idasanutlin) is observed.

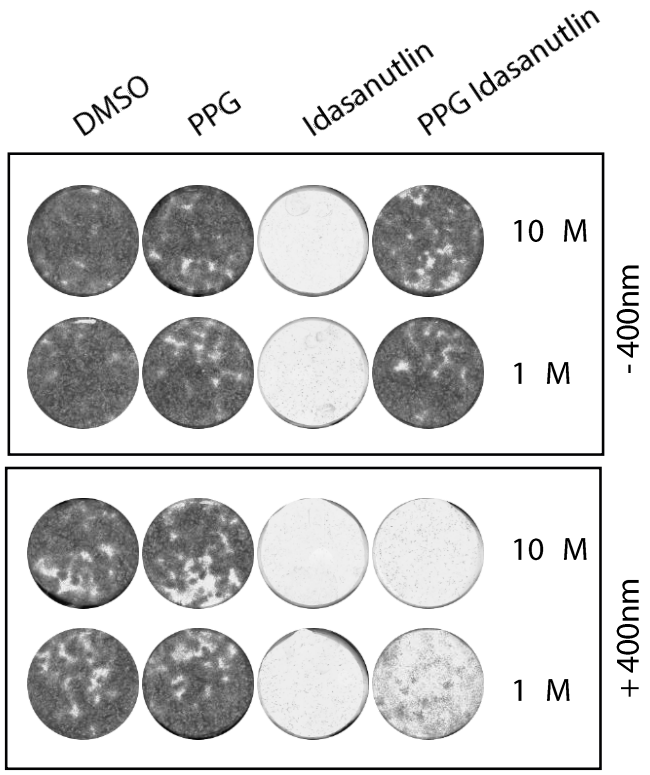

Figure S15: Cell outgrowth experiments showing that PPG 6 (the photoproduct after photocleavagedoes not perturb cellular outgrowth.

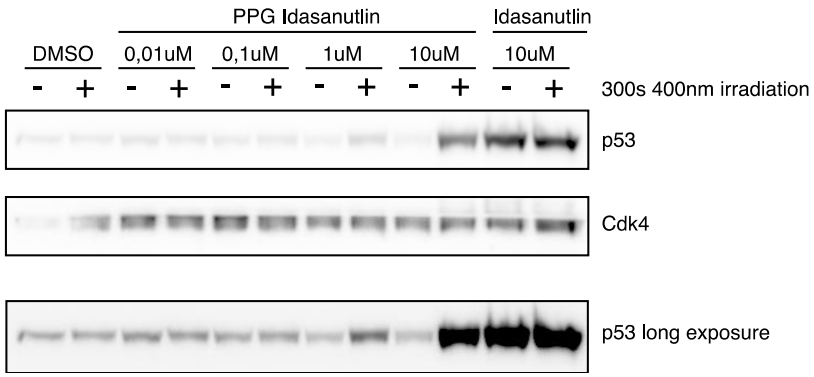

Figure S16: Representative western blot showing the dose-dependent p53 stabilization in RPE-1 cells after indicated treatments.

References

(1) Montalti, M.; Credi, A.; Prodi, L.; Gandolfi, M. T.; Michl, J.; Balzani, V. *Handbook of Photochemistry*, Third Edition, (CRC Press, 2006).

(2) Hatchard, C. G.; Parker, C. A. A New Sensitive Chemical Actinometer. II. Potassium Ferrioxalate as a Standard Chemical Actinometer. *Proc. R. Soc. A Math. Phys. Eng. Sci.* **1956**, *235*, 518–536.

(3) Loewer, A.; Batchelor, E.; Gaglia, G.; Lahav, G. Basal Dynamics of P53 Reveal Transcriptionally Attenuated Pulses in Cycling Cells. *Cell* **2010**, *142*, 89–100.

(4) Lindström, S.; Eriksson, M.; Vazin, T.; Sandberg, J.; Lundeberg, J.; Frisén, J.; Andersson-Svahn, H. High-Density Microwell Chip for Culture and Analysis of Stem Cells. *PLoS One* **2009**, *4*, e6997.

(5) Feringa, F. M.; Krenning, L.; Koch, A.; van den Berg, J.; van den Broek, B.; Jalink, K.; Medema, R. H. Hypersensitivity to DNA Damage in Antephase as a Safeguard for Genome Stability. *Nat. Commun.* **2016**, *7*, 12618.

(6) Ding, Q.; Zhang, Z.; Liu, J.-J.; Jiang, N.; Zhang, J.; Ross, T. M.; Chu, X.-J.; Bartkovitz, D.; Podlaski, F.; Janson, C.; Tovar, C.; Filipovic, Z. M.; Higgins, B.; Glenn, K.; Packman, K.; Vassilev, L. T.; Graves, B. Discovery of RG7388, a Potent and Selective P53–MDM2 Inhibitor in Clinical Development. *J. Med. Chem.* **2013**, *56*, 5979–5983.

(7) Shu, L.; Li, Z.; Gu, C.; Fishlock, D. Synthesis of a Spiroindolinone Pyrrolidinecarboxamide MDM2 Antagonist. *Org. Process Res. Dev.* **2013**, *17*, 247–256.

(8) Szymański, W.; Velema, W. A.; Feringa, B. L. Photocaging of Carboxylic Acids: A Modular Approach. *Angew. Chem., Int. Ed.* **2014**, *53*, 8682–8686.

(9) Gandioso, A.; Cano, M.; Massaguer, A.; Marchan, V. A Green Light-Triggerable RGD Peptide for Photocontrolled Targeted Drug Delivery: Synthesis and Photolysis Studies. *J. Org. Chem.* **2016**, *81*, 11556–11564.